ATLAS NOTE

ATL-PHYS-PUB-2016-002

11th January 2016

Multi-boson simulation for 13 TeV ATLAS analyses

The ATLAS Collaboration

Abstract

This note describes the Monte Carlo setup used by ATLAS to model multi-boson processes in 13 TeV pp collisions. The baseline Monte Carlo generators are compared with each other in key kinematic distributions of the processes under study. Sample normalization and assignment of systematic uncertainties are discussed.

1 Introduction

Measurements of diboson production at the Large Hadron Collider (LHC) provide an excellent test of the electroweak sector in the Standard Model (SM). The production of multiple heavy gauge bosons V ($= W^{\pm}, Z$) opens up a multitude of potential decay channels categorized according to the number of charged leptons in the final state. Numerous Monte Carlo tools exist to simulate the various multi-boson production processes involving additional jets.

This note documents the Monte Carlo setup used by ATLAS to model multi-boson processes in proton-proton collisions at a center-of-mass energy of 13 TeV. The note is organized as follows. The baseline generators employed throughout are first introduced in Section 2. The fully leptonic diboson processes are described in Section 3, semi-leptonic diboson processes are discussed in Section 6 and loop-induced diboson processes are covered in Section 5. Diboson processes involving electroweak dijet production (such as vector boson scattering) are then considered in Section 4 and, finally, triboson processes (VVV) are dealt with in Section 7.

2 Baseline generators

The two baseline generators being studied are Sherpa and Powheg. As the former is evolving rapidly, several versions are investigated in parallel.

Sherpa [1] is a parton shower Monte Carlo generator simulating additional hard parton emissions [2] that are matched to a parton shower based on Catani-Seymour dipoles [3]. The NLO+PS matching [4] is employed for different jet multiplicities which are then merged into an inclusive sample using the MEPS@NLO approach [5]. The following versions of Sherpa have been employed:

- Sherpa v2.2.0 with the authors' default tune for this version and NNPDF3.0 NNLO parton density functions [6] as well as the authors' default tune for multiple parton interactions. For NLO matrix elements, virtual QCD corrections are provided by the OpenLoops v1.2.0 library [7] using the Collier tensor integral reduction library [8].
- Sherpa v2.1.1 with the authors' default tune for this version and CT10 NLO parton density functions [9] as well as the authors' default tune for multiple parton interactions. For NLO matrix elements, virtual QCD corrections are provided by the OpenLoops library.
- Sherpa v1.4.5 with the authors' default tune for this version and CT10 parton density functions as well as the authors' default tune for multiple parton interactions. This version of Sherpa can only calculate matrix elements at leading order (LO) accuracy.

PowhegBox [10–12] provides a general framework for implementing NLO QCD calculations with shower Monte Carlo programs based on the Powheg method. A library of processes is available which can be interfaced with shower Monte Carlo programs through the Les Houches Interface [13, 14]. In this note, PowhegBox v2 interfaced to PYTHIA v8.210 [15] for parton showering is used.

In addition, other dedicated generators have been used for certain signatures. These shall be introduced in the relevant sections.

3 Fully leptonic diboson processes

This section describes fully leptonic processes of the type $qq \to VV$, where both V bosons decay leptonically (including all lepton flavors, where τ leptons subsequently can decay leptonically or hadronically). The processes are grouped according to the number of charged leptons, giving rise to the following final states: 4ℓ, $3\ell\nu$, $2\ell 2\nu$, $\ell 3\nu$ and 4ν. Note that the lepton charges in the $2\ell 2\nu$ are of opposite sign. A dedicated sample for the $2\ell 2\nu jj$ final state, where the two lepton charges are of equal sign, has been generated as well.

3.1 Generator setup

3.1.1 Sherpa

Matrix elements for the fully leptonic diboson processes have been generated using Sherpa v2.1.1 with up to three additional partons in the final state. The 4ℓ and $2\ell 2\nu$ decay modes include NLO matrix elements for configurations with up to one additional parton at matrix-element level, whereas the $3\ell\nu$, $\ell 3\nu$ and 4ν decay modes include NLO accurate matrix elements for the inclusive process only. All other parton configurations are LO accurate. The same-sign $2\ell 2\nu jj$ matrix elements are only LO accurate with up to one additional parton. A generator-level cut of 5 GeV on the transverse momentum of the two highest-p_{T} leptons is imposed for all samples. Furthermore, the dilepton invariant mass $m_{\ell\ell}$ is required to exceed $2m_{\ell}$ + 250 MeV. The $2\ell 2\nu$ final state has been generated without bottom quarks in the hard scattering process, to avoid contributions from top-quark mediated processes.

The ME+PS method clusters the hard scattering multi-parton configurations to define a shower-like history, which affects the initial conditions of the parton shower as well as the calculated core scale, since the latter depends on the inverted process. The option METS_CLUSTER_MODE=16 has been used in all samples (except the same-sign $2\ell 2\nu$ one) generated with Sherpa v2.1.1 to allow for unordered histories, which brings the performance of the clustering algorithm closer to the default used in Sherpa v2.2.0. Furthermore, EXCLUSIVE_CLUSTER_MODE has been enabled for all samples (including same-sign $2\ell 2\nu$), ensuring that only QCD splittings are inverted by the clustering algorithm, thus allowing for the leptons to be associated with the core process. The Sherpa default scale setting approach is used.

3.1.2 Powheg

PowhegBox v2 is used to generate the WW, WZ and ZZ [16, 17] processes to NLO precision in QCD. The samples are split according to final-state, charged lepton multiplicity (4ℓ, $3\ell\nu$, $2\ell 2\nu$, $\ell 3\nu$, 4ν). However, each sample is inclusive regarding the lepton flavor. All final-states include the effect of off-shell singly resonant amplitudes, and the WZ and ZZ samples include the effects of Z/γ^* interference. Interference effects due to identical leptons in the final state are included as well, but are ignored between WW and ZZ for the common decay mode to same-flavor opposite-charge leptons and a pair of neutrinos – a negligible effect at Born level [16].

Samples are generated using PowhegBox v2, base revision r3033. The specific PowhegBox process version is r2819 for each diboson (WW, WZ, ZZ) sample. Events are generated using the CT10 NLO [9] PDF and then showered with PYTHIA8 using the AZNLO [18] tune and the CTEQ6L1 [19] PDF for the shower. The EvtGen [20] afterburner is used to ensure that heavy quarks are properly decayed. The dynamic scale

of the mass of the boson pair is used for both the factorization and renormalization scales. The `withdamp` and `bornzerodamp` flags were set in `PowhegBox` for each sample to ensure that any phase-space region in which the Born cross section vanishes is properly handled.

A matrix element level generator cut is placed on the Z boson decay products in the case that they are charged leptons, requiring the mass of the charged lepton pair to be greater than 4 GeV. If there are two Z bosons decaying to like-flavored charged leptons, the cut is applied to the two possible pairings.

3.2 Cross sections

Since both `PowhegBox` and `Sherpa` sample cross sections are already evaluated at NLO precision in QCD, the predicted cross sections are directly used for sample normalization. A summary is given in tables 1 and 2. Note that `Sherpa` considers processes by final state, including diboson mixtures, whereas `Powheg+PYTHIA8` is broken down by individual VV processes. The minimum requirement on the dilepton mass described in section 3.1.2, which is required for the `Powheg` samples at the generator level (but not for the `Sherpa` samples), leads to large differences in the predicted cross sections. Furthermore, it should be noted that NNLO QCD calculations start to become available for VV production incorporating leptonic V decays along with spin correlations as well as off-shell effects [21], resulting in non-negligible cross section enhancements. The first such result for the ZZ process was utilized as reference in the first measurement of the ZZ production cross section at $\sqrt{s} = 13$ TeV by ATLAS [22].

Table 1: Summary of the generator cross sections at $\sqrt{s} = 13$ TeV predicted by `Sherpa` for fully leptonic diboson final states.

Final state	`Sherpa` (pb)
4ℓ	11.69
$3\ell\nu$	11.88
$2\ell 2\nu$	12.74
$\ell 3\nu$	3.094
4ν	0.600
$2\ell 2\nu jj$	0.024

The normalization of the `Sherpa` predictions includes a correction to account for different electroweak schemes. `Sherpa` is using an electroweak parameter scheme were $\alpha_{\mathrm{QED}}(m_Z)$ and the boson masses are used as input and the other parameters are calculated from the corresponding tree-level relations. This can lead to values of e.g. the weak mixing angle which deviate from the PDG values, or also differences to the α_{QED} calculated in the G_μ scheme. Since the inclusive cross section of the diboson samples with their four electroweak vertices is particularly affected by this discrepancy, it has been decided to scale down the `Sherpa` predictions by a factor of 0.91 which roughly accounts for this difference.

Table 2: Summary of the generator cross sections at $\sqrt{s}$ = 13 TeV predicted by Powheg+PYTHIA8 for fully leptonic diboson final states.

Final state	Powheg (pb)
$ZZ \to 4\ell$	1.267
$WZ \to 3\ell\nu$	4.502
$WW \to 2\ell 2\nu$	10.63
$ZZ \to 2\ell 2\nu$	0.918
$WZ \to \ell 3\nu$	2.778
$ZZ \to 4\nu$	0.549

3.3 Systematic uncertainties

3.3.1 MCFM uncertainties

The MCFM [23, 24] Monte Carlo program allows the evaluation of NLO cross section predictions for a variety of processes at hadron colliders as well as LO (lhe) event generation for a subset of these processes. The NLO cross sections for 13 TeV WW, WZ and ZZ production with fully leptonic decay modes are evaluated using MCFM v7.0.1 with CT10 NLO PDF and a dynamic scale of $m_{VV}/2$ for renormalization and factorization scales. The Z boson mass range evaluated is $66 - 116$ GeV, and non-resonant $gg \to WW$ and $gg \to ZZ$ production is included at LO. Scale uncertainties are derived using the maximum and minimum values when varying renormalization and factorization scales independently by factors of two. The resulting uncertainties are found to be at the 4–5 % level, depending on the process under study. CT10 PDF uncertainties are derived from the eigenvector error sets as described in [25] and scaled to 68 % CL, yielding an $\approx$ 2% uncertainty for the processes studied. Adding both uncertainties in quadrature, a (conservative) uncertainty of 6 % is used for the total NLO WW, WZ and ZZ production cross sections.

The MCFM cross sections are only used to evaluate the systematic uncertainties as detailed above and not to normalize the samples discussed in this section. Since the generators of these samples already have NLO accuracy themselves, their native cross sections are used.

3.3.2 Explicit variations for the Sherpa samples

Explicit scale variations have been generated for each of the fully leptonic diboson final states. These include variations of the factorization scale μ_f, the renormalization scale μ_r, the resummation scale μ_q as well as the CKKW merging scale. A summary is provided in table 3.

Table 3: Summary of the systematic variations considered for the Sherpa samples of fully leptonic diboson final states. These include variations of the factorization scale μ_f, the renormalization scale μ_r, the resummation scale μ_q as well as the CKKW merging scale.

	Factorization scale		Renormalization scale		Resummation scale		CKKW scale	
Final state	$2\mu_f$	$0.5\mu_f$	$2\mu_r$	$0.5\mu_r$	$2\mu_q$	$0.5\mu_q$	15 GeV	30 GeV
4ℓ	×	×	×	×	×	×		
$3\ell\nu$	×	×	×	×	×	×	×	×
$2\ell 2\nu$	×	×	×	×	×	×	×	×
$\ell 3\nu$	×	×	×	×	×	×		
4ν	×	×	×	×	×	×		
$2\ell 2\nu jj$	×	×	×	×	×	×		

3.3.3 On-the-fly variations for the Powheg samples

To enable studies of systematic uncertainties due to PDF and scale variations, the PowhegBox samples were generated including weights corresponding to:

- independent variations of renormalization and factorization scales by a factor of two (nine variations including the nominal scale settings),

- PDF variations for the `CT10 NLO` [9] eigenvector error sets (52 variations) and central values of `MSTW2008nlo` [26], `NNPDF3.0` [6] PDFs.

3.4 Generator comparisons

In the following we provide validation plots with different object definitions and event selections. Where jets are used, they are reconstructed using the anti-k_t clustering algorithm [27] with a jet-radius parameter of $R = 0.4$. The jet transverse momentum is required to be greater than 30 GeV. The distance between jets and leptons is required to be $\Delta R_{\ell j} > 0.1$ in η-ϕ space. In case of overlap, the jet is removed if $E_\ell / E_{\text{jet}} > 0.5$, otherwise the lepton is removed. Leptons are dressed with photons in a cone of $\Delta R_{\ell j} < 0.1$ centered on the lepton. Photons originating from quarks are ignored. Moreover, photons are assigned to their nearest lepton in η-ϕ space in order to avoid double counting. In case more than one lepton combination satisfies the reconstruction criteria of the boson candidates, the product of probabilities according to the relevant Breit-Wigner distribution (W or Z) is maximized.

Further details of the selections are given in the respective subsections. Note that all shown uncertainties are statistical only and, moreover, that the shown plots are for a center-of-mass energy of 8 TeV rather than 13 TeV, as their purpose was to compare the improved `Sherpa v2.1` against the Run I setup, which made use of the old `Sherpa v1.4`.

3.4.1 4ℓ final state

The comparison has been done in a phase space designed for the `Powheg` samples, since it was not possible to impose a kinematic selection for particles originating from the matrix element.

- leptons with same flavor and opposite charge
- leptons $p_{\text{T}} > 10$ GeV, $m_{\ell\ell} > 10$ GeV

Figure 1 shows comparisons between `Powheg+PYTHIA8` and `Sherpa` in the 4ℓ final state. All curves are normalized to the predicted cross section of their respective generator. Curves corresponding to `Sherpa v1.4` are scaled to the `Sherpa v2.1` prediction in order to account for NLO corrections. `Powheg+PYTHIA8` and `Sherpa v2.1` show less events with no or one jet compared to `Sherpa v1.4`. For high jet multiplicities `Sherpa` predicts larger rates compared to `Powheg+PYTHIA8`, in line with the expectation that a simple NLO+PS setup is not sufficient to describe multi-jet configurations. Other variables show a good agreement between `Powheg+PYTHIA8` and `Sherpa v2.1`, while `Sherpa v1.4` is slightly off, e.g. in the dilepton mass spectrum and in the lepton p_{T} spectrum below 30 GeV. The Z-boson candidate containing the hardest lepton is referred to as Z_1.

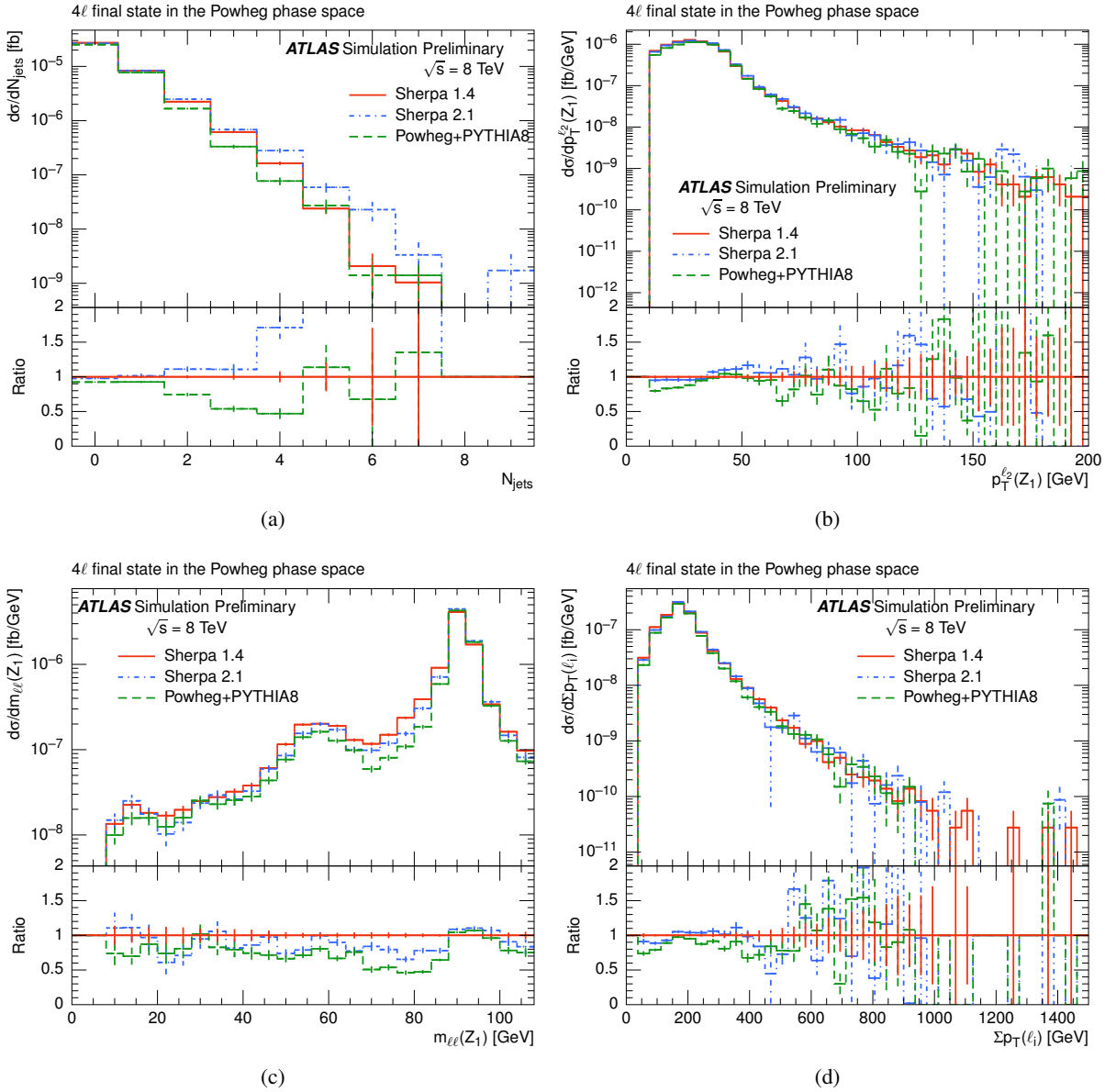

Figure 1: Comparisons of (a) the jet multiplicity, (b) the sub-leading lepton p_{T} distribution for the Z-boson candidate with the hardest lepton (Z_1), (c) the dilepton mass spectrum for Z_1 and (d) the summed lepton p_{T} using `Powheg+PYTHIA8` and `Sherpa`. Curves corresponding to `Sherpa v1.4` are scaled to the `Sherpa v2.1` prediction in order to account for NLO corrections. Uncertainties are statistical only, ratios are with respect to the first curve mentioned in the legend.

3.4.2 $3\ell\nu$ final state

The comparison has been done in two different phase spaces. The first phase space is as inclusive as possible. All kinematic selections are supposed to mimic the generator-level selection and have been implemented to select a common phase space:

- leptons with same flavor and opposite charge,
- leptons $p_{\mathrm{T}} > 5$ GeV, $|\eta| < 2.7$, $m_{\ell\ell} > 5$ GeV

As it is not possible to impose a kinematic selection for particles originating from the matrix element in `Powheg`, the `Sherpa` samples have instead been adapted to the `Powheg` definition by imposing the kinematic requirements on leptons coming from the matrix element (HEPMC status 3). This gives rise to the `Powheg` phase space:

- leptons with same flavor and opposite charge
- leptons $p_{\mathrm{T}} > 10$ GeV, $m_{\ell\ell} > 10$ GeV

Figures 2–4 show comparisons between `Powheg+PYTHIA8` and `Sherpa` in the $3\ell\nu$ final state. All curves are normalized to the predicted cross section of their respective generator. Curves corresponding to `Sherpa v1.4` are scaled to the `Sherpa v2.1` prediction in order to account for NLO corrections. `Sherpa` again predicts larger rates than `Powheg+PYTHIA8` for higher jet multiplicities due to its full incorporation of multi-jet matrix elements. In addition, `Sherpa v2.1` exhibits a forward excess in the jet activity, which is known to the authors and has been improved upon in newer versions. The `Powheg+PYTHIA8` sample shows more central jets. The discrepancies in the jet pseudorapidity (due to the known `Sherpa` excess in forward activity) also lead to deviations in e.g. the dijet mass spectrum or the jet rapidity difference. Furthermore, a strange dip has been observed for `Powheg+PYTHIA8` in the summed lepton p_{T} distribution around 500 GeV.

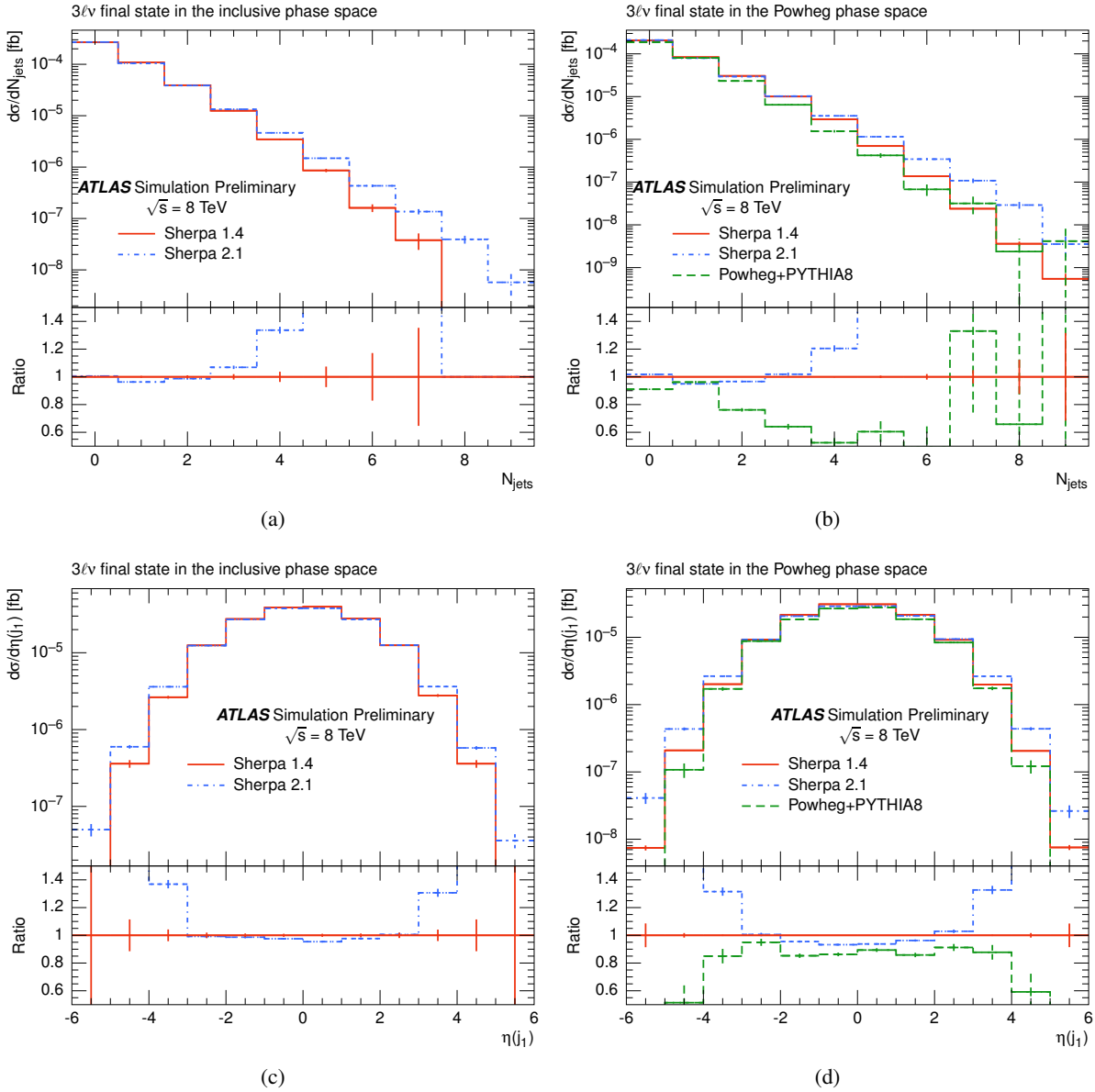

Figure 2: Comparisons of the jet multiplicity (top row) and the leading jet pseudorapidity distribution (bottom row) between different versions of `Sherpa` in the inclusive region (on the left) as well as between `Sherpa` and `Powheg+PYTHIA8` in the `Powheg` phase space (on the right). Curves corresponding to `Sherpa v1.4` are scaled to the `Sherpa v2.1` prediction in order to account for NLO corrections. Uncertainties are statistical only, ratios are with respect to the first curve mentioned in the legend.

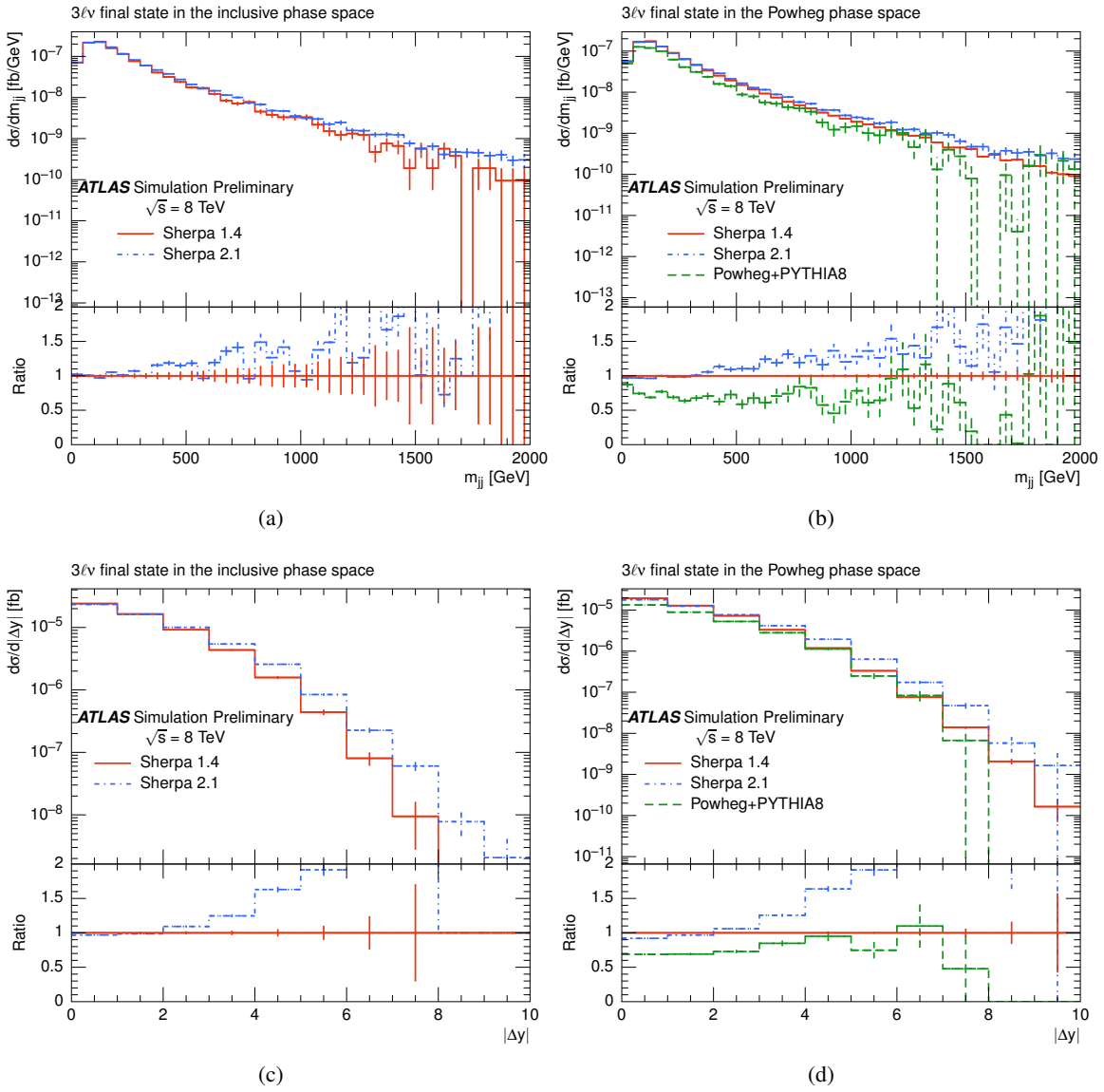

Figure 3: Comparisons of the dijet mass spectrum (top row) and the jet rapidity difference (bottom row) between different versions of `Sherpa` in the inclusive phase space (on the left) as well as between `Sherpa` and `Powheg+PYTHIA8` in the `Powheg` phase space (on the right). Curves corresponding to `Sherpa v1.4` are scaled to the `Sherpa v2.1` prediction in order to account for NLO corrections. Uncertainties are statistical only, ratios are with respect to the first curve mentioned in the legend.

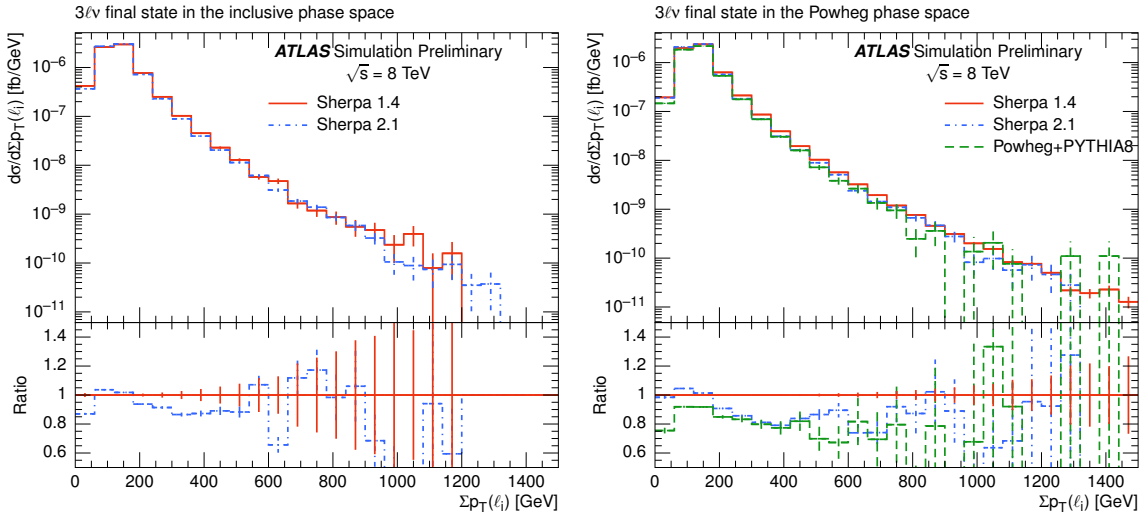

(a) (b)

Figure 4: Comparisons of the summed lepton p_{T} distribution between different versions of `Sherpa` in the inclusive phase space (on the left) as well as between `Sherpa` and `Powheg+PYTHIA8` in the `Powheg` phase space (on the right). Curves corresponding to `Sherpa v1.4` are scaled to the `Sherpa v2.1` prediction in order to account for NLO corrections. Uncertainties are statistical only, ratios are with respect to the first curve mentioned in the legend.

3.4.3 Opposite-sign $2\ell 2\nu$ final state

The comparison has been done in two different phase spaces. The first phase space is as inclusive as possible. All kinematic selections are supposed to mimic the generator-level selection and have been implemented to select a common phase space:

- leptons with same flavor and opposite charge
- leptons $p_{\mathrm{T}} > 5$ GeV, $|\eta| < 2.7$, $m_{\ell\ell} > 5$ GeV

As it is not possible to impose a kinematic selection for particles originating from the matrix element in `Powheg`, the `Sherpa` samples have instead been adapted to the `Powheg` definition by imposing the kinematic requirements on leptons coming from the matrix element (HEPMC status 3). This gives rise to the `Powheg` phase space:

- leptons with same flavor and opposite charge
- leptons $p_{\mathrm{T}} > 10$ GeV, $m_{\ell\ell} > 10$ GeV

Figures 5–7 show comparisons between `Powheg+PYTHIA8` and `Sherpa` in the opposite-sign $2\ell 2\nu$ final state. The samples include also the ZZ component for that final state, which can be seen in the lepton-pair mass distribution. The `Sherpa` samples even include the interference between all diagrams (WW and ZZ) leading to this final state, which could explain why there are differences with respect to the `Powheg` samples in the ZZ peak region. All curves are normalized to the predicted cross section of their respective generator. Curves corresponding to `Sherpa v1.4` are scaled to the `Sherpa v2.1` prediction in order to account for NLO corrections. `Sherpa v2.1` shows higher jet multiplicities starting with two jets. In addition, a forward excess of jets has been observed. On the other hand, `Powheg+PYTHIA8` undershoots in the region of the Z-boson resonance. The forward excess of jets leads to discrepancies in other variables as well, e.g. the dijet rapidity difference, the dijet invariant mass or the summed jet p_{T} distribution.

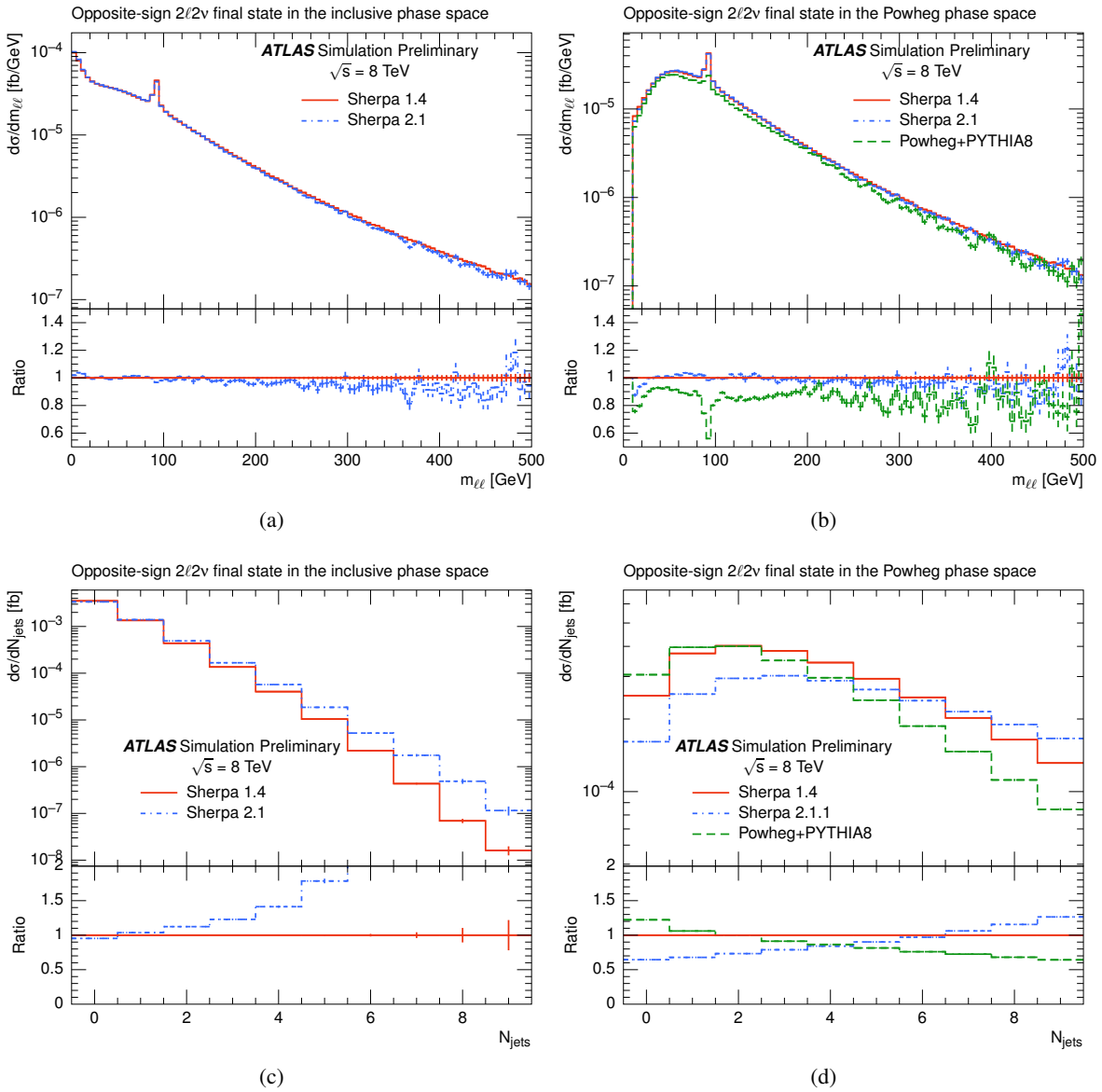

Figure 5: Comparisons of the dilepton mass spectrum (top row) and the jet multiplicity (bottom row) between different versions of `Sherpa` in the inclusive region (on the left) as well as between `Sherpa` and `Powheg+PYTHIA8` in the `Powheg` region (on the right). Curves corresponding to `Sherpa v1.4` are scaled to the `Sherpa v2.1` prediction in order to account for NLO corrections. Uncertainties are statistical only, ratios are with respect to the first curve mentioned in the legend.

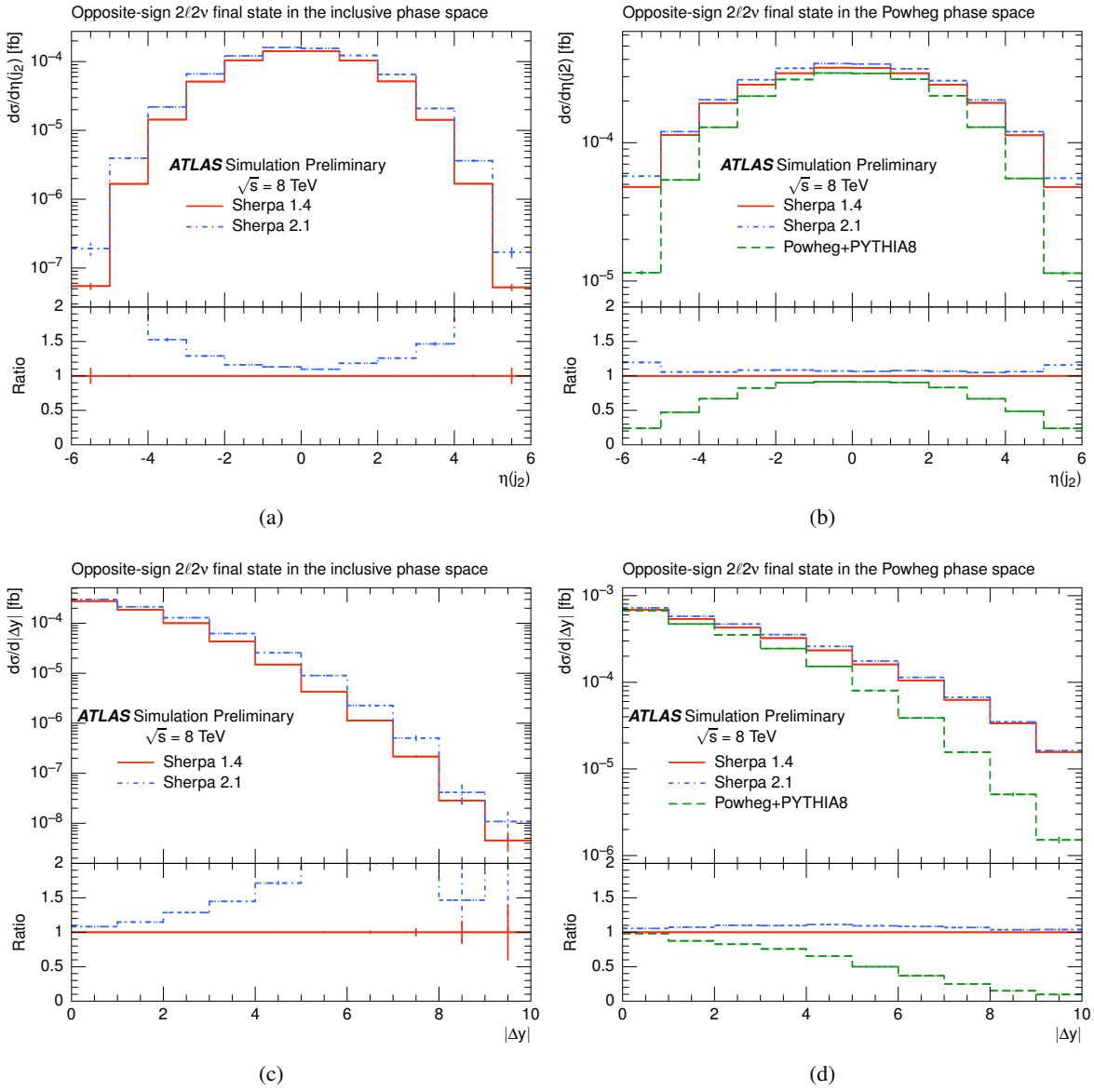

Figure 6: Comparisons of the sub-leading jet pseudorapidity distribution (top row) and the jet rapidity difference (bottom row) between different versions of `Sherpa` in the inclusive region (on the left) as well as between `Sherpa` and `Powheg+PYTHIA8` in the `Powheg` region (on the right). Curves corresponding to `Sherpa v1.4` are scaled to the `Sherpa v2.1` prediction in order to account for NLO corrections. Uncertainties are statistical only, ratios are with respect to the first curve mentioned in the legend.

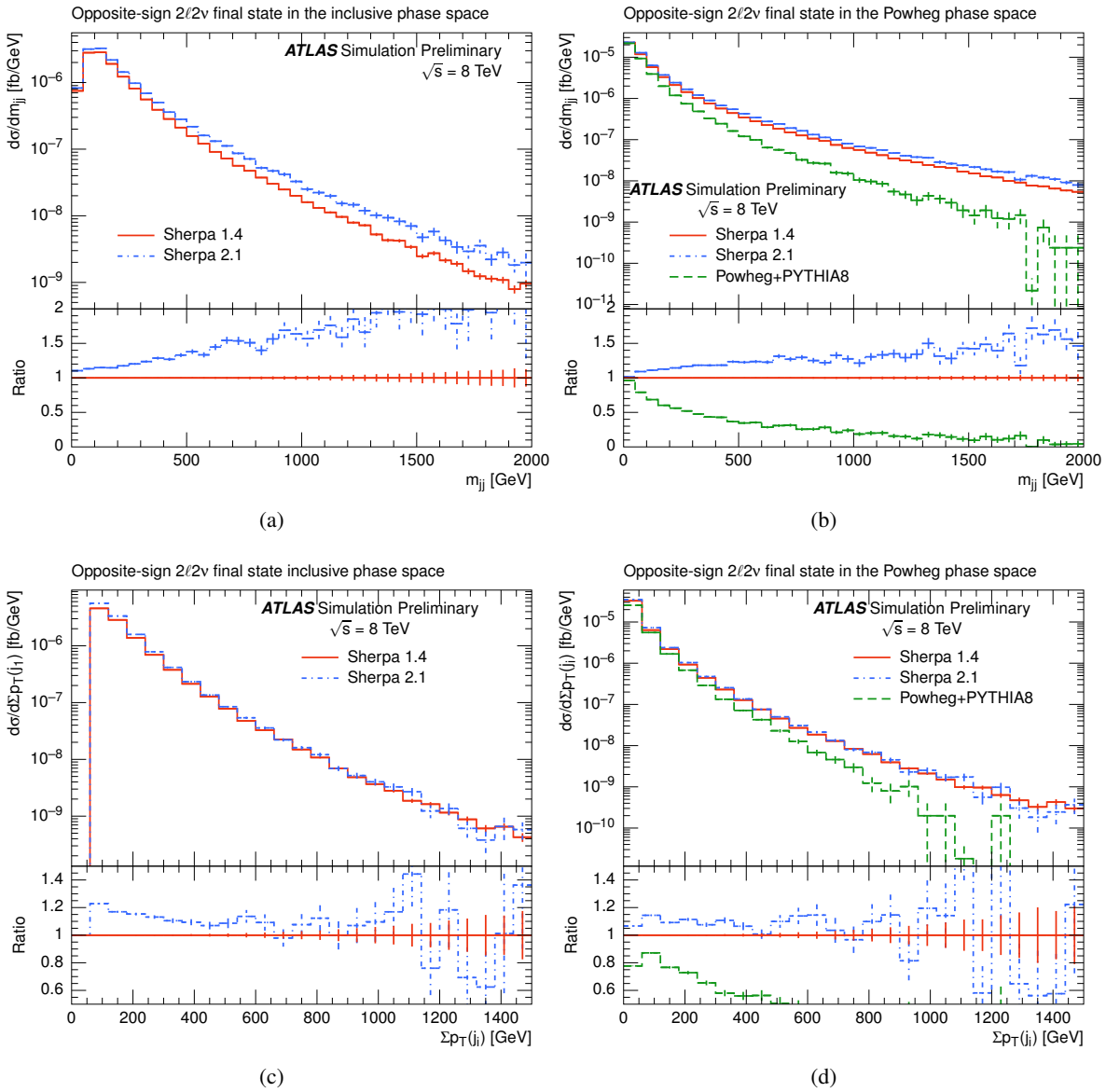

Figure 7: Comparisons of the dijet invariant mass spectrum (top row) and the summed jet p_{T} distribution (bottom row) between different versions of `Sherpa` in the inclusive region (on the left) as well as between `Sherpa` and `Powheg+PYTHIA8` in the `Powheg` region (on the right). Curves corresponding to `Sherpa v1.4` are scaled to the `Sherpa v2.1` prediction in order to account for NLO corrections. Uncertainties are statistical only, ratios are with respect to the first curve mentioned in the legend.

3.4.4 Same-sign $2\ell 2\nu$ final state

The comparison has been done in two different phase spaces. The first phase space is as inclusive as possible. All kinematic selections are supposed to mimic the generator-level selection and have been implemented to select a common phase space:

- leptons coming from a matrix element (HEPMC status 3)
- leptons with same flavor and same charge
- leptons $p_{\mathrm{T}} > 5$ GeV, $m_{\ell\ell} > 0.1$ GeV

The second phase space is a signal region optimized for the vector boson scattering (VBS) process. For the same-sign WW process it is defined as:

- leptons coming from a matrix element (HEPMC status 3)
- leptons with same flavor and same charge
- leptons $p_{\mathrm{T}} > 5$ GeV, $m_{\ell\ell} > 20$ GeV
- at least 2 jets, $m_{jj} > 500$ GeV, $\Delta R_{jj} > 0.4$
- τ-veto
- exactly two leptons with $|\eta| < 2.5$, $p_{\mathrm{T}} > 20.0$ GeV
- third lepton e/μ veto if $p_{\mathrm{T}} > 7.0/6.0$ GeV
- $\Delta R_{\ell j} > 0.3$
- $\Delta R_{\ell\ell} > 0.3$
- $E_{\mathrm{T}}^{\mathrm{miss}} > 40$ GeV
- $|\Delta y_{jj}| > 2.4$

Figures 8–11 show comparisons between different versions of `Sherpa` in the same-sign $2\ell 2\nu$ final state. All curves are normalized to the predicted cross section of their respective generator. Curves corresponding to `Sherpa v1.4` are scaled to the `Sherpa v2.1` prediction in order to account for NLO corrections. `Sherpa v2.1` shows more jets for higher jet multiplicities starting with six jets in the inclusive phase space. Furthermore, the known `Sherpa` excess in the forward jet activity can be seen, which leads to flaws in other variables, e.g. the dijet mass spectrum or the jet rapidity. These discrepancies are much reduced in the VBS signal region though. In addition to the forward excess of jets, `Sherpa v2.1` shows a harder summed jet p_{T} distribution as well as more central leptons, which is also seen in other variables, e.g. the lepton pseudorapidity difference. All discrepancies are reduced again in the VBS signal phase space. The new `Sherpa` samples also show a softer diboson mass spectrum and a higher summed lepton p_{T} distribution.

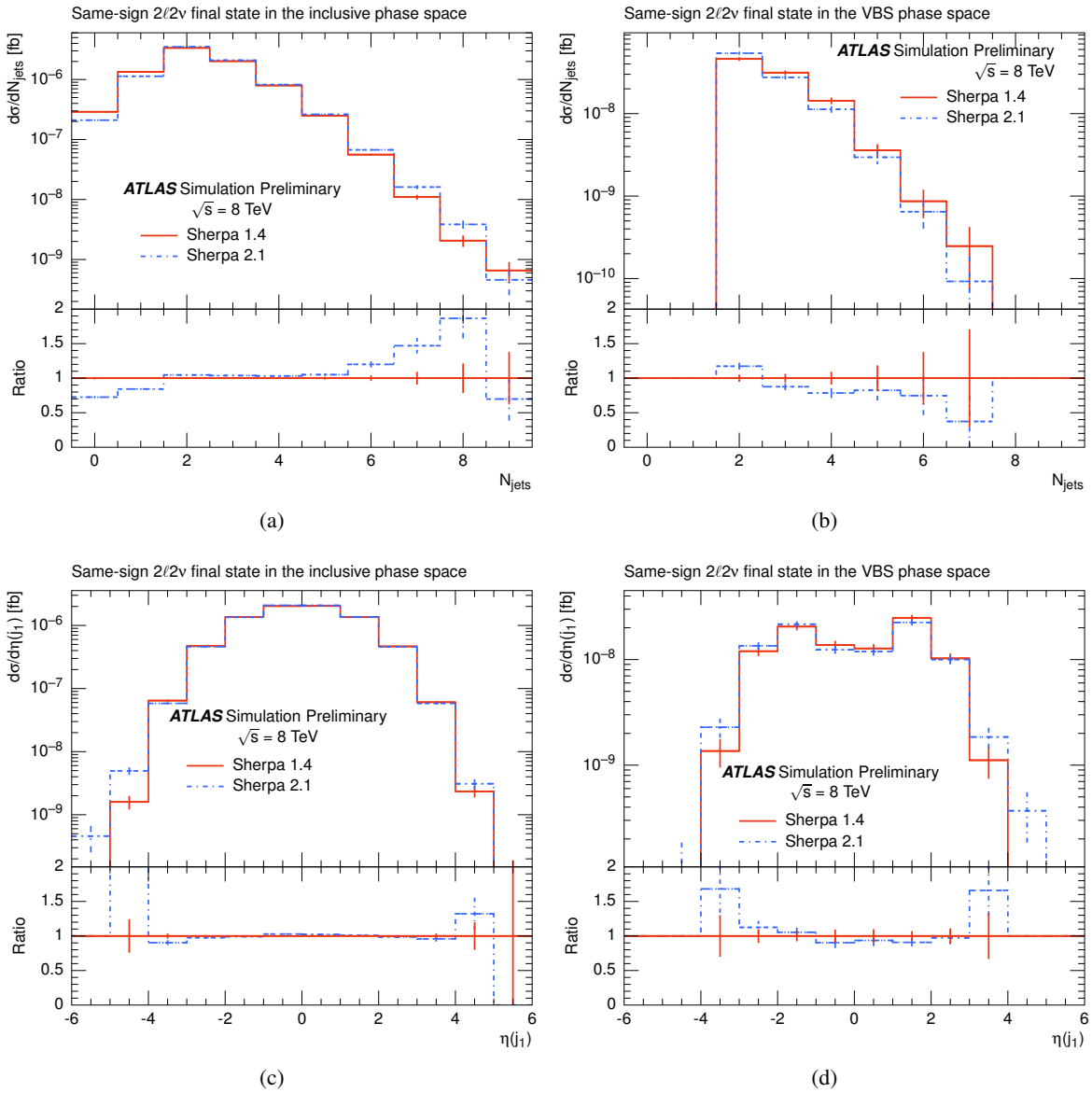

Figure 8: Comparisons of the jet multiplicity (top row) and the leading jet rapidity distribution (bottom row) between different versions of `Sherpa` in the inclusive region (on the left) as well as the VBS signal region (on the right). Curves corresponding to `Sherpa v1.4` are scaled to the `Sherpa v2.1` prediction in order to account for NLO corrections. Uncertainties are statistical only, ratios are with respect to the first curve mentioned in the legend.

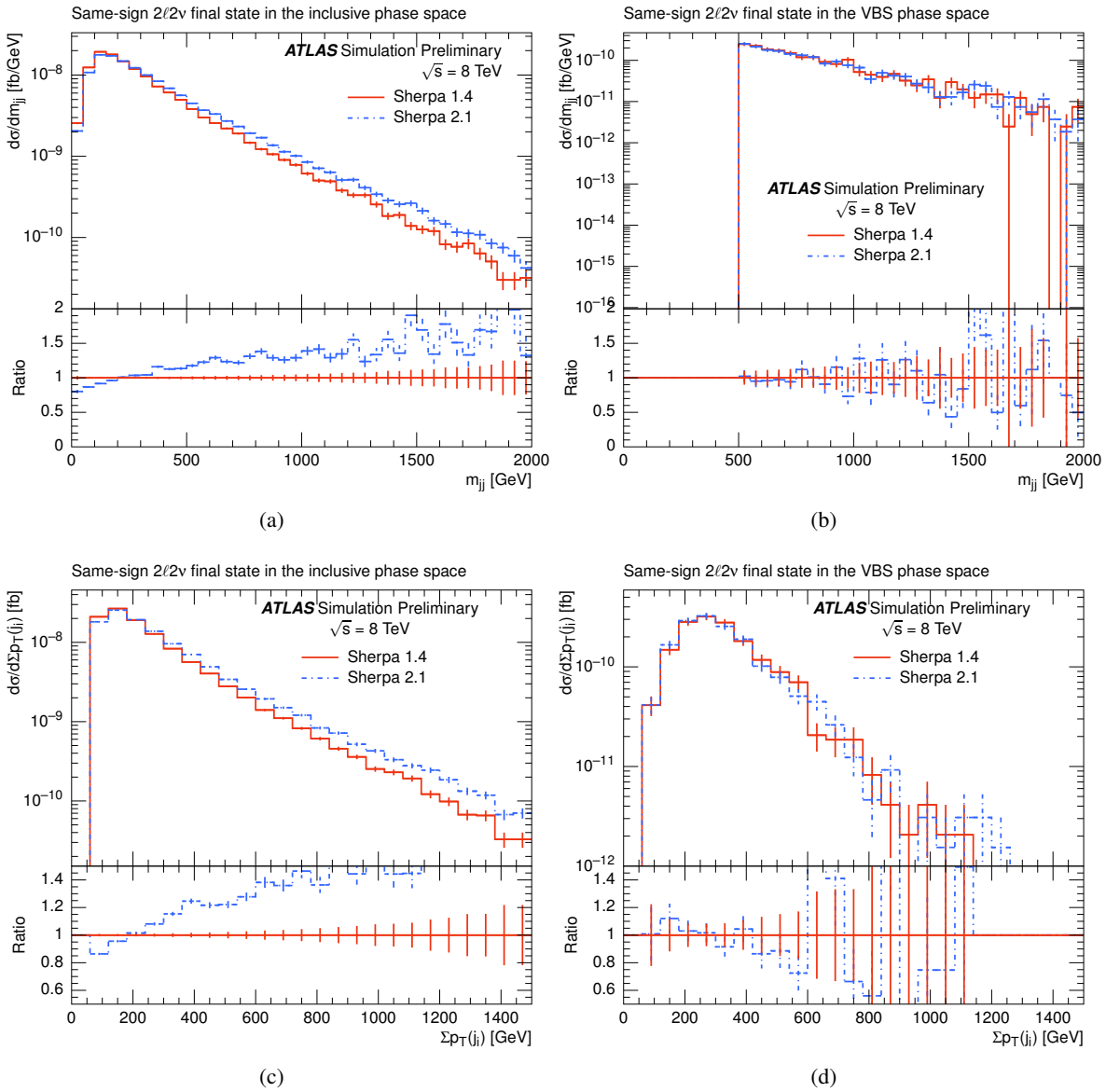

Figure 9: Comparisons of the invariant mass spectrum (top row) and the the summed jet p_{T} distribution (bottom row) between different versions of `Sherpa` in the inclusive region (on the left) as well as the VBS signal region (on the right). Curves corresponding to `Sherpa v1.4` are scaled to the `Sherpa v2.1` prediction in order to account for NLO corrections. Uncertainties are statistical only, ratios are with respect to the first curve mentioned in the legend.

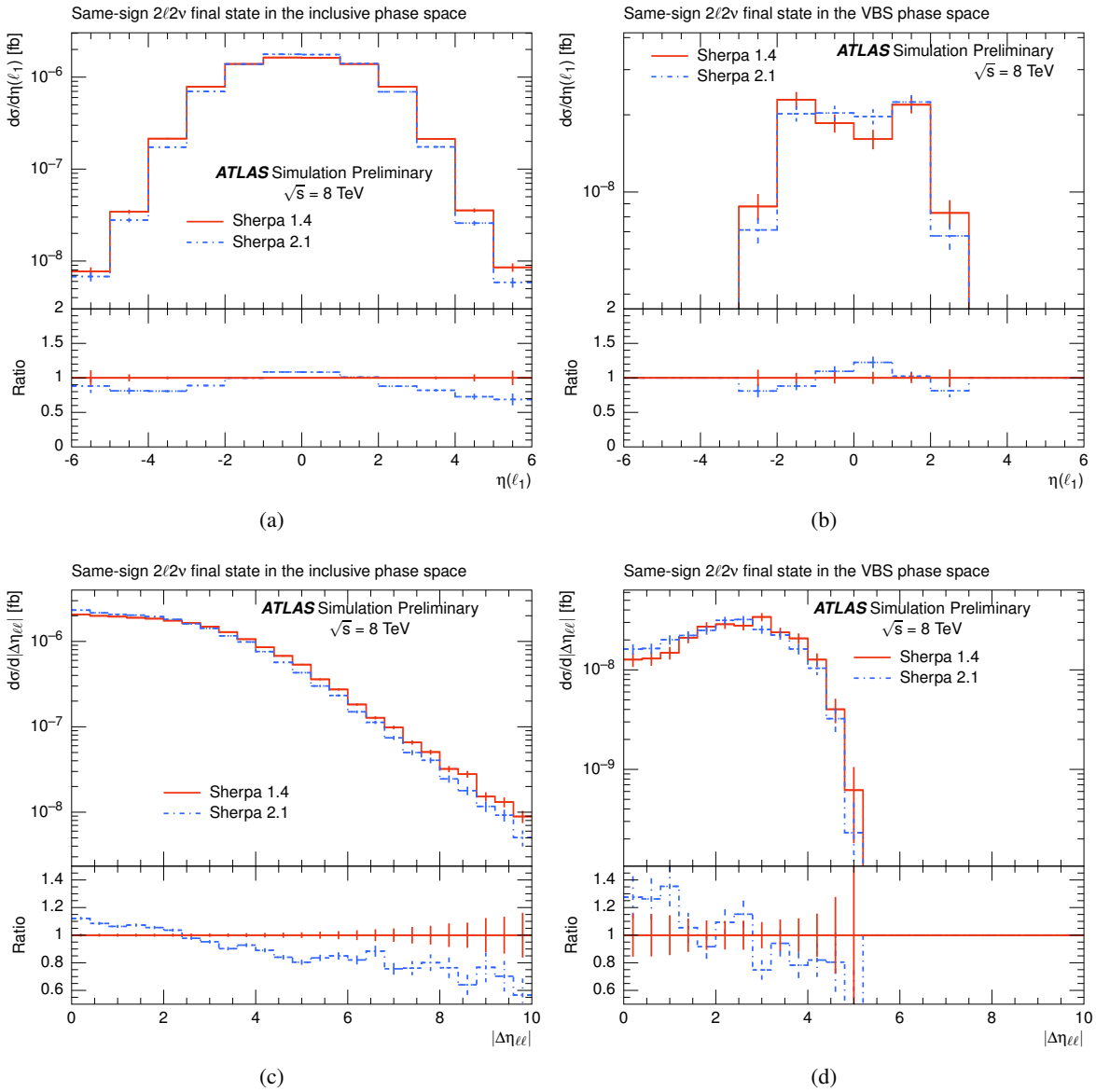

Figure 10: Comparisons of the leading lepton pseudorapidity distribution (top row) and the lepton rapidity difference (bottom row) between different versions of `Sherpa` in the inclusive region (on the left) as well as the VBS signal region (on the right). Curves corresponding to `Sherpa v1.4` are scaled to the `Sherpa v2.1` prediction in order to account for NLO corrections. Uncertainties are statistical only, ratios are with respect to the first curve mentioned in the legend.

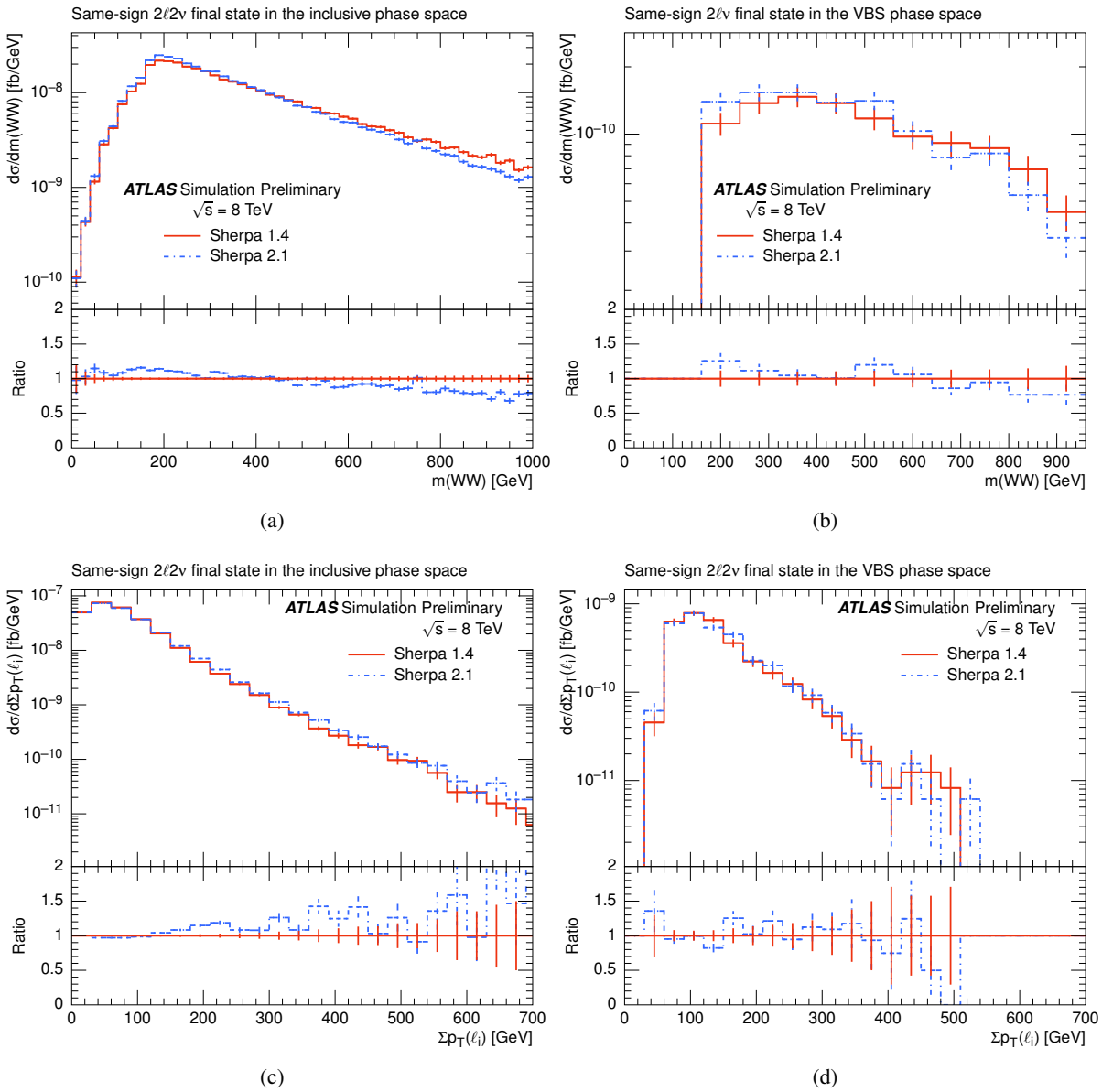

Figure 11: Comparisons of the diboson invariant mass spectrum (top row) and the summed lepton p_{T} distribution (bottom row) between different versions of `Sherpa` in the inclusive region (on the left) as well as the VBS signal region (on the right). Curves corresponding to `Sherpa v1.4` are scaled to the `Sherpa v2.1` prediction in order to account for NLO corrections. Uncertainties are statistical only, ratios are with respect to the first curve mentioned in the legend.

4 Electroweak diboson processes

Dedicated samples for the gauge-invariant set of electroweak processes involving the vector boson scattering (VBS) diagram have been generated. For these processes the jets recoil against the heavy gauge boson, giving rise to an extra two electroweak couplings. This includes the $3\ell\nu jj$ and $4\ell jj$ final states as well as the $2\ell 2\nu jj$ final state, where the two lepton charges are of equal sign.

4.1 Generator setup

4.1.1 Sherpa

Matrix elements for the electroweak $3\ell\nu jj$, $4\ell jj$ as well as same-sign $2\ell 2\nu jj$ processes have been generated at LO accuracy using `Sherpa v2.1.1` with up to one additional parton in the final state. The nominal factorisation scale has been set to the invariant mass of the diboson system. Further details of the general `Sherpa` setup are provided in section 2.

4.2 Cross sections

4.2.1 Generator cross sections

A summary of the cross sections predicted by Sherpa is given in table 4.

Table 4: Summary of the generator cross sections at $\sqrt{s} = 13$ TeV predicted by Sherpa for electroweak diboson final states.

Final state	Sherpa prediction (pb)
$4\ell jj$	0.029
$3\ell\nu jj$	0.038
$2\ell 2\nu jj$	0.039

The normalization of the Sherpa predictions includes a correction to account for different electroweak schemes. Sherpa is using an electroweak parameter scheme were $\alpha_{\text{QED}}(m_Z)$ and the boson masses are used as input and the other parameters are calculated from the corresponding tree-level relations. This can lead to values of e.g. the weak mixing angle which deviate from the PDG values, or also differences to the α_{QED} calculated in the G_μ scheme. Since the inclusive cross section of the diboson samples with their four electroweak vertices is particularly affected by this discrepancy, it has been decided to scale down the Sherpa predictions by a factor of 0.91 which roughly accounts for this difference.

4.3 Generator comparisons

In the following we provide validation plots with different object definitions and event selections. Where jets are used, they are reconstructed using the anti-k_t clustering algorithm [27] with a jet-radius parameter of $R = 0.4$. Further details of the selections are given in the respective subsections. Note that all shown uncertainties are statistical only and, moreover, that the shown plots are for a center-of-mass energy of 8 TeV rather than 13 TeV, as their purpose was to compare the improved Sherpa v2.1 against the Run I setup, which made use of the old Sherpa v1.4.

4.3.1 Same-sign $2\ell 2\nu jj$ final state

The jet transverse momentum is required to be greater than 30 GeV. The distance between jets and leptons is required to be $\Delta R_{\ell j} > 0.1$ in η-ϕ space. In case of overlap, the jet is removed if $E_\ell / E_{\text{jet}} > 0.5$, otherwise the lepton is removed. Leptons are dressed with photons in a cone of $\Delta R_{\ell j} < 0.1$ centered on the lepton. Photons originating from quarks are ignored. Moreover, photons are assigned to their nearest lepton in η-ϕ space in order to avoid double counting. In case more than one lepton combination satisfies the reconstruction criteria of the boson candidates, the product of probabilities according to the relevant Breit-Wigner distribution (W or Z) is maximized.

The comparison has been done in two different phase spaces. The first phase space is as inclusive as possible. All kinematic selections are supposed to mimic the generator-level selection and have been implemented to select a common phase space:

- leptons coming from a matrix element (HEPMC status 3)

- leptons with same flavor and opposite charge
- leptons $p_{\mathrm{T}} > 5$ GeV, $m_{\ell\ell} > 0.1$ GeV

The second phase space is a signal region optimized for VBS. For the same-sign WW process it is defined as:

- leptons coming from a matrix element (HEPMC status 3)
- leptons $p_{\mathrm{T}} > 5$ GeV, $m_{\ell\ell} > 20$ GeV
- at least 2 jets, $m_{jj} > 500$ GeV, $\Delta R_{jj} > 0.4$
- τ-veto
- exactly two leptons with $|\eta| < 2.5$, $p_{\mathrm{T}} > 20$ GeV
- third lepton e/μ veto if $p_{\mathrm{T}} > 7.0/6.0$ GeV
- $\Delta R_{\ell j} > 0.3$
- $\Delta R_{\ell\ell} > 0.3$
- $E_{\mathrm{T}}^{\mathrm{miss}} > 40$ GeV
- $|\Delta y_{jj}| > 2.4$

Figures 12 and 13 show comparisons between different versions of `Sherpa` in the same-sign $2\ell 2\nu jj$ final state. All curves are normalized to the predicted cross section of their respective generator. Curves corresponding to `Sherpa v1.4` are scaled to the `Sherpa v2.1` prediction in order to account for NLO corrections. The `Sherpa v2.1` samples tend to be softer than those using the old version of `Sherpa`. Furthermore, the summed lepton p_{T} distribution shows significant differences between the versions. This also leads to a softer diboson invariant mass spectrum. However, within the statistical uncertainties, the agreement is much better in the VBS region. Moreover, the new sample shows significantly more jets in both phase spaces.

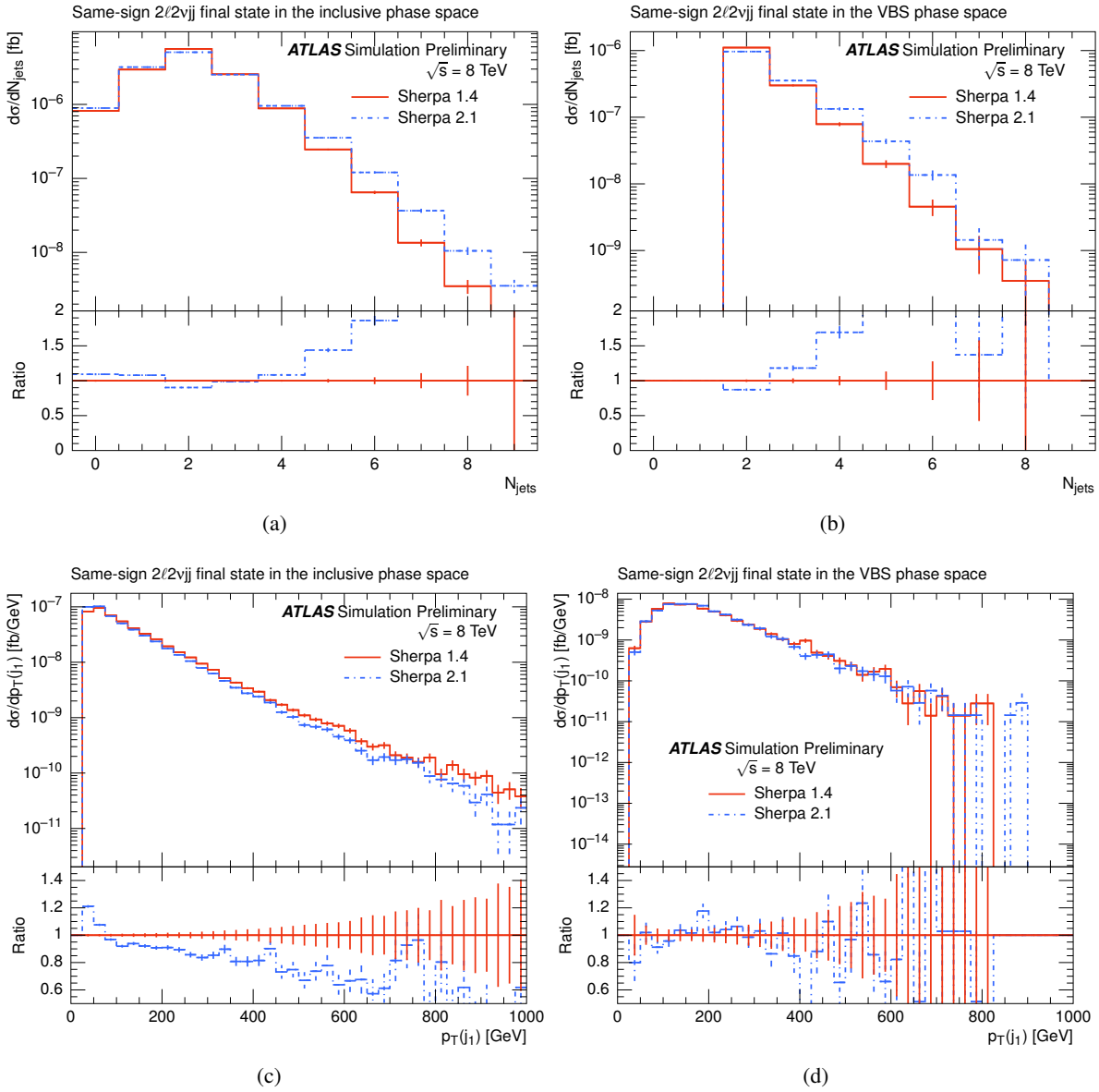

Figure 12: Comparisons of the jet multiplicity (top row) and the leading jet p_{T} spectrum (bottom row) between different versions of `Sherpa` in the inclusive region (on the left) as well as the VBS signal region (on the right). Curves corresponding to `Sherpa v1.4` are scaled to the `Sherpa v2.1` prediction in order to account for NLO corrections. Uncertainties are statistical only, ratios are with respect to the first curve mentioned in the legend.

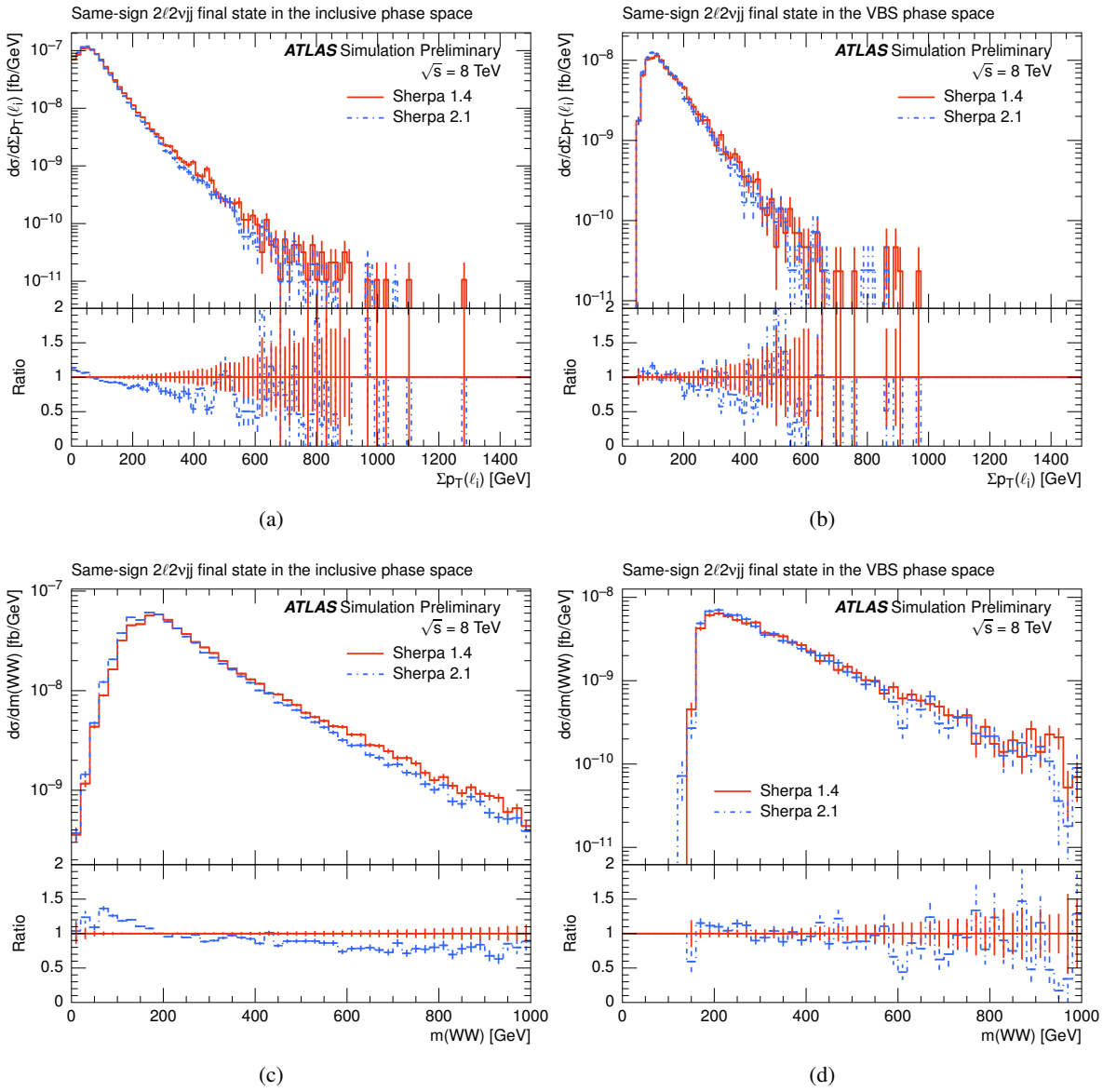

Figure 13: Comparisons of the the summed lepton p_{T} distribution (top row) and the diboson invariant mass spectrum (bottom row) between different versions of `Sherpa` in the inclusive region (on the left) as well as the VBS signal region (on the right). Curves corresponding to `Sherpa v1.4` are scaled to the `Sherpa v2.1` prediction in order to account for NLO corrections. Uncertainties are statistical only, ratios are with respect to the first curve mentioned in the legend.

4.3.2 $3\ell\nu jj$ final state

The jet transverse momentum is required to be greater than 30 GeV. The distance between jets and leptons is required to be $\Delta R_{\ell j} > 0.1$ in η-ϕ space. In case of overlap, the jet is removed if $E_\ell / E_{\text{jet}} > 0.5$, otherwise the lepton is removed. Leptons are dressed with photons in a cone of $\Delta R_{\ell j} < 0.1$ centered on the lepton. Photons originating from quarks are ignored. Moreover, photons are assigned to their nearest lepton in η-ϕ space in order to avoid double counting. In case more than one lepton combination satisfies the reconstruction criteria of the boson candidates, the product of probabilities according to the relevant Breit-Wigner distribution (W or Z) is maximized.

The comparison has been done in two different phase spaces. The first phase space is as inclusive as possible. All kinematic selections are supposed to mimic the generator-level selection and have been implemented to select a common phase space:

- leptons coming from a matrix element (HEPMC status 3)
- leptons with same flavor and opposite charge
- leptons $p_{\text{T}} > 10$ GeV, $|\eta| < 2.7$, $m_{\ell\ell} > 5$ GeV
- veto on matrix-element b

The second phase space is a signal region optimized for VBS. For the WZ process it is defined as:

- leptons coming from a matrix element (HEPMC status 3)
- leptons $p_{\text{T}} > 5$ GeV, $|\eta| < 2.5$, $m_{\ell\ell} > 5$ GeV
- at least 2 jets, $m_{jj} > 500$ GeV, $\Delta R_{jj} > 0.4$
- b-veto, τ-veto
- For the W-boson candidate: Lepton $p_{\text{T}} > 20$ GeV, $\Delta R_{\ell j} > 0.3$, $\Delta R_{\ell\ell} > 0.3$
- For the Z-boson candidate: Lepton $p_{\text{T}} > 15$ GeV, $\Delta R_{\ell j} > 0.2$, $\Delta R_{\ell\ell} > 0.2$
- $m_{\text{T}}(W) > 30$ GeV

Figures 14 and 15 show comparisons between different versions of `Sherpa` in the $3\ell\nu jj$ final state. All curves are normalized to the predicted cross section of their respective generator. Curves corresponding to `Sherpa v1.4` are scaled to the `Sherpa v2.1` prediction in order to account for NLO corrections. The electroweak samples show very different behavior in the forward region. In the newer `Sherpa` version the jets tend to be more central which affects other distributions as well, e.g. the jet rapidity difference or the dijet invariant jet mass. All discrepancies are much reduced in the VBS phase space. The new sample shows significantly more jets in both phase spaces.

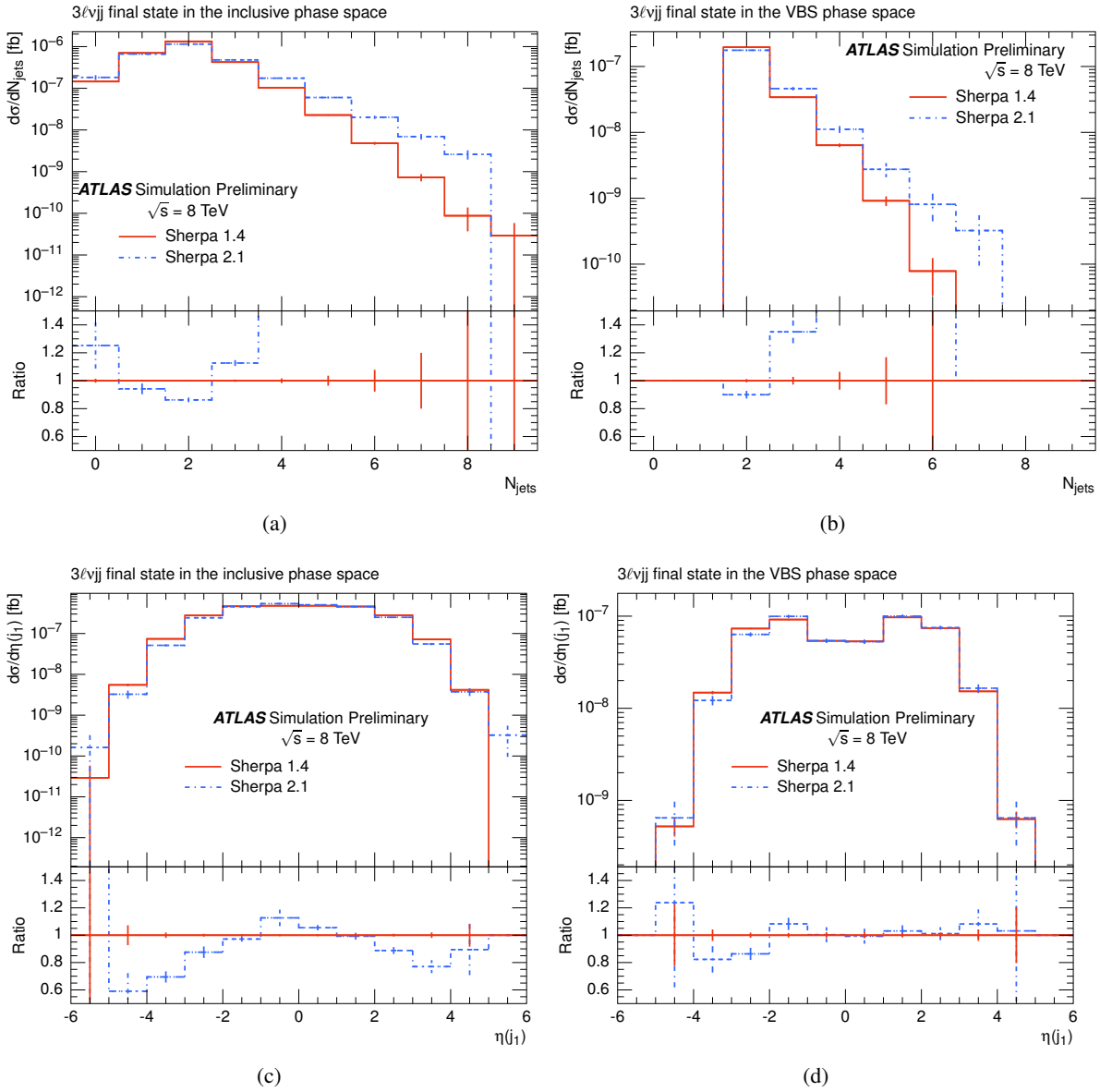

Figure 14: Comparisons of the jet multiplicity (top row) and the leading jet pseudorapidity spectrum (bottom row) between different versions of `Sherpa` in the inclusive region (on the left) as well as the VBS signal region (on the right). Curves corresponding to `Sherpa v1.4` are scaled to the `Sherpa v2.1` prediction in order to account for NLO corrections. Uncertainties are statistical only, ratios are with respect to the first curve mentioned in the legend.

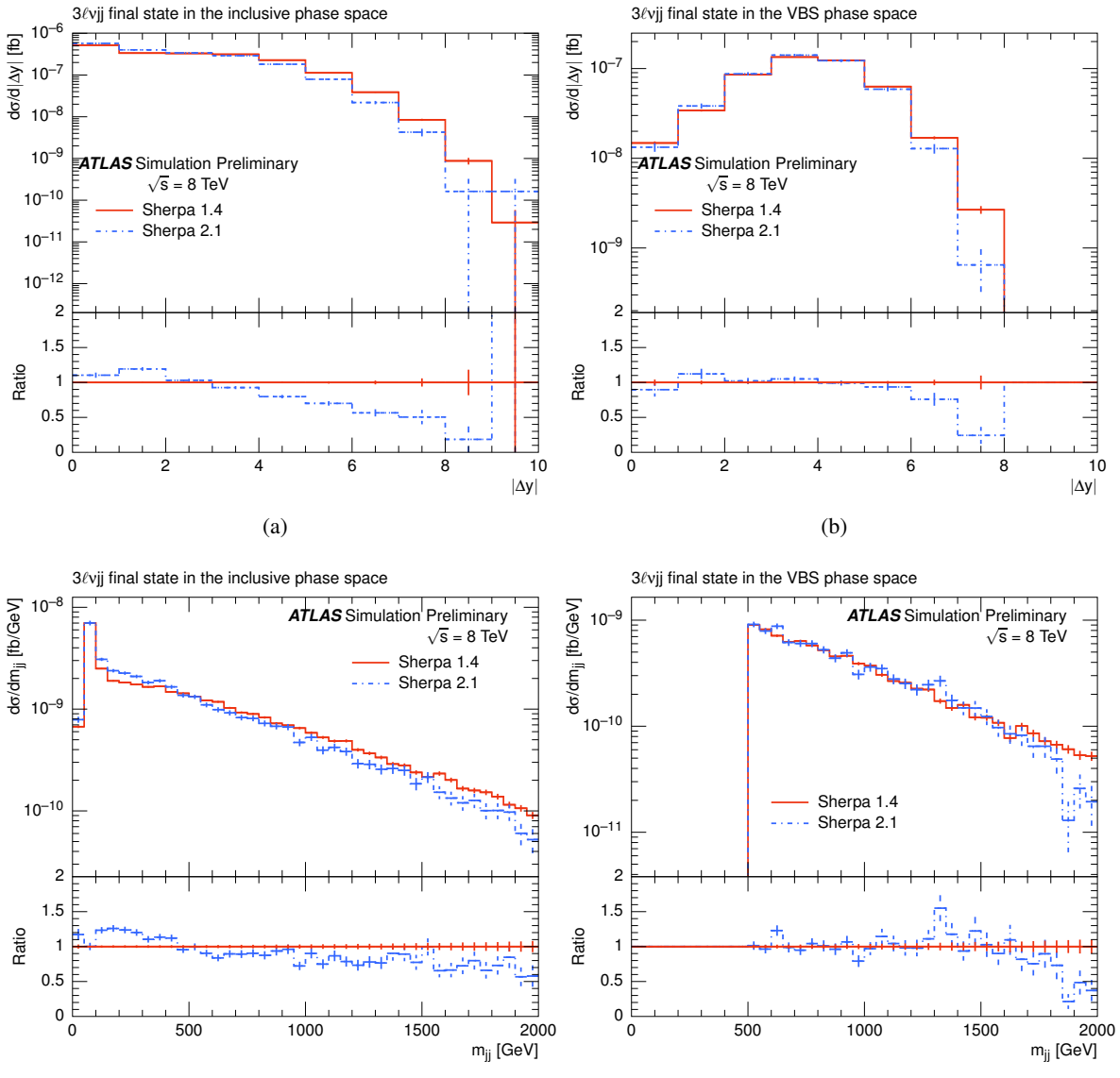

Figure 15: Comparisons of the jet rapidity difference (top row) and the dijet invariant mass spectrum (bottom row) between different versions of `Sherpa` in the inclusive region (on the left) as well as the VBS signal region (on the right). Curves corresponding to `Sherpa v1.4` are scaled to the `Sherpa v2.1` prediction in order to account for NLO corrections. Uncertainties are statistical only, ratios are with respect to the first curve mentioned in the legend.

5 Loop-induced diboson processes

Loop-induced processes are of the type $gg \to VV$ where both of the bosons decay leptonically. Dedicated samples have been generated for the 4ℓ and $2\ell 2\nu$ final states, which includes $gg \to H$ diagrams.

5.1 Generator setup

5.1.1 Sherpa

Matrix elements for the loop-induced diboson processes have been generated using OpenLoops within Sherpa v2.1.1 with up to one additional parton in the final state. The matrix elements are LO accurate. These are generated in the spirit of [28] and thus contain not only on-shell $gg \to VV$ production, but the fully leptonic final state including all off-shell/interference effects.

The EXCLUSIVE_CLUSTER_MODE has been enabled for all samples, ensuring that only QCD splittings are inverted by the clustering algorithm, thus allowing for the leptons to be associated with the core process. This core process is then used to set the core scale $\mu = m_{VV}/2$ within the scale setting approach used by Sherpa.

5.1.2 gg2VV

The generator gg2VV v3.1.6 [29, 30] was used to produce samples with the final states 4ℓ and $2\ell 2\nu$. The matrix element is calculated at leading order, including diagrams with the Standard Model Higgs as an intermediate particle. The Higgs width predicted by the Standard Model is used and off-shell effects are properly taken into account as well. Furthermore, all possible interferences, like the final-state-lepton interference for four same-flavor charged leptons or the ZZ/WW interference for same-flavor $2\ell 2\nu$ are taken into account. In most cases the generator is configured to use the CT10 leading order PDF set, and the dynamic renormalization and factorization scale $m(VV)$. For special applications there are deviations from this baseline configuration.

Finally, since gg2VV is a leading order generator, the default showering performed by PYTHIA8 needed to be adjusted. Studies on jet distributions showed too hard a spectrum for the common configuration used by ATLAS. Therefore it is altered with the option SpaceShower:pTmaxMatch = 1 (so called "wimpy shower") which showed more reasonable agreement with previous Monte Carlo samples showered with HERWIG [31], according distributions based on Sherpa and data.

5.2 Cross sections

5.2.1 Generator cross sections

A summary of the cross sections predicted by Sherpa and gg2VV is given in table 5.

The normalization of the Sherpa predictions includes a correction to account for different electroweak schemes. Sherpa is using an electroweak parameter scheme were $\alpha_{\mathrm{QED}}(m_Z)$ and the boson masses are used as input and the other parameters are calculated from the corresponding tree-level relations. This

Table 5: Summary of the generator cross sections at $\sqrt{s} = 13$ TeV predicted by Sherpa and gg2VV+PYTHIA8 for loop-induced diboson final states. Note that the generator-level setup is not identical between the two, so some differences are expected.

	Predicted cross sections	
Final state	Sherpa (pb)	gg2VV (pb)
4ℓ	0.019	0.011
$2\ell 2\nu$	0.777	—

can lead to values of e.g. the weak mixing angle which deviate from the PDG values, or also differences to the α_{QED} calculated in the G_μ scheme. Since the inclusive cross section of the diboson samples with their four electroweak vertices is particularly affected by this discrepancy, it has been decided to scale down the Sherpa predictions by a factor of 0.91 which roughly accounts for this difference.

5.3 Systematic uncertainties

5.3.1 Explicit variations for the Sherpa samples

Explicit scale variations have been generated for each of the semi-leptonic diboson final states. These include variations of the factorization scale μ_{f}, the renormalization scale μ_{r} as well as the resummation scale μ_{q} – each by a factor of 2 and 0.5, respectively.

6 Semi-leptonic diboson processes

This section describes semi-leptonic processes of the type $qq \to VV$, where only one of the V bosons decays leptonically (including all lepton flavors, where τ leptons subsequently can decay leptonically or hadronically), whilst the other one decays hadronically, giving rise to the following final states: $W(\to \ell\nu)W(\to qq)$, $W(\to \ell\nu)Z(\to qq)$, $Z(\to \ell\ell)W(\to qq)$, $Z(\to \nu\nu)W(\to qq)$, $Z(\to \ell\ell)Z(\to qq)$, and $Z(\to \nu\nu)Z(\to qq)$.

6.1 Generator setup

6.1.1 Sherpa

Matrix elements for the semi-leptonic diboson processes have been generated using Sherpa v2.1.1 with up to three additional partons in the final state. The two ZZ decay modes include NLO matrix elements for configurations with up to one additional parton at matrix-element level, whereas the WZ and WW decay modes include NLO accurate matrix elements for the inclusive process only. All other parton configurations are LO accurate. In addition, the two WW final states have been generated without bottom quarks in the hard scattering process, to avoid contributions from top-quark mediated processes.

The ME+PS method clusters the hard scattering multi-parton configurations to define a shower-like history, which affects the initial conditions of the parton shower as well as the calculated core scale, since the latter depends on the inverted process. The option METS_CLUSTER_MODE=16 has been used in all samples generated with Sherpa v2.1.1 to allow for unordered histories, which brings the performance of the clustering algorithm closer to the default used in Sherpa v2.2.0. Furthermore, EXCLUSIVE_CLUSTER_MODE has been enabled for all samples, ensuring that only QCD splittings are inverted by the clustering algorithm, thus allowing for the vector bosons to be associated with the core process. This core process is then used to set the core scale $\mu = m_{VV}/2$ within the scale setting approach used by Sherpa.

6.1.2 Powheg

PowhegBox v2 is used to generate WW, WZ and ZZ samples to NLO precision in QCD. The samples are split according to semi-leptonic final-states ($2\ell qq$, $\ell\nu qq$, $2\nu qq$). However, each sample is inclusive regarding the lepton flavor. NLO corrections to the hadronic decay processes are not included, but the hadronic V decays are generally well modeled by showering Monte Carlos. All final-states include the effect of off-shell singly resonant amplitudes, and the WZ and ZZ samples include the effects of Z/γ^* interference.

Samples are generated using PowhegBox v2, base revision r3033. The specific PowhegBox process version is r2819 for each diboson (WW, WZ, ZZ) sample. Events are generated using the CT10 NLO [9] PDF and then showered with PYTHIA8 using the AZNLO [18] tune and the CTEQ6L1 [19] PDF for the shower. The EvtGen [20] afterburner is used to ensure that heavy quarks are properly decayed. The dynamic scale of the mass of the boson pair is used for both the factorization and renormalization scales. The withdamp and bornzerodamp flags were set in PowhegBox for each sample to ensure that any phase-space region in which the Born cross section vanishes is properly handled.

A matrix element level generator cut is placed on the Z boson decay products in the case that they are charged leptons or quarks, requiring the mass of the charged lepton or quark pair to be greater than 20 GeV.

6.2 Cross sections

6.2.1 Generator cross sections

Since both PowhegBox and Sherpa sample cross sections are already evaluated at NLO precision in QCD, the predicted cross sections are directly used for sample normalization. A summary is given in table 6 for the nominal samples. Note that the generator-level setup is not identical between PowhegBox and Sherpa so some differences are expected.

Predictions for the $W(\to \ell\nu)Z(\to qq)$ final state are available from both Sherpa v2.1.1 and v2.2.0. The cross section values are 10.460 pb and 10.099 pb, respectively, thus showing good agreement between both generator versions. More detailed comparisons of kinematic distributions are presented in section 6.4.2.

Table 6: Summary of the generator cross sections at $\sqrt{s} = 13$ TeV predicted by Sherpa and Powheg+PYTHIA8 for semi-leptonic diboson final states.

	Predicted cross sections	
Final state	Sherpa (pb)	Powheg (pb)
$W(\to \ell\nu)W(\to qq)$	45.27	44.18
$W(\to \ell\nu)Z(\to qq)$	10.46	10.10
$Z(\to \ell\ell)W(\to qq)$	3.12	3.28
$Z(\to \nu\nu)W(\to qq)$	6.17	5.77
$Z(\to \ell\ell)Z(\to qq)$	2.14	2.27
$Z(\to \nu\nu)Z(\to qq)$	4.22	3.94

The normalization of the Sherpa predictions includes a correction to account for different electroweak schemes. Sherpa is using an electroweak parameter scheme were $\alpha_{\text{QED}}(m_Z)$ and the boson masses are used as input and the other parameters are calculated from the corresponding tree-level relations. This can lead to values of e.g. the weak mixing angle which deviate from the PDG values, or also differences to the α_{QED} calculated in the G_μ scheme. Since the inclusive cross section of the diboson samples with their four electroweak vertices is particularly affected by this discrepancy, it has been decided to scale down the Sherpa predictions by a factor of 0.91 which roughly accounts for this difference. Note that for the Sherpa 2.2.0 samples, the EW parameters and branching ratios of the vector bosons have been adjusted, such that they comply with the PDG values and no subsequent scaling is necessary.

6.3 Systematic uncertainties

6.3.1 MCFM uncertainties

To cross check the systematic uncertainties derived for fully leptonic decay modes in Section 3.3.1, MCFM was run using the WW process as test bench with identical settings, except switching to hadronic decays for the W^+ or the W^- boson. Again, the used uncertainty of 6 % is found to cover the uncertainties due to scale and PDF variations added in quadrature.

It should be noted however, that it was not possible to evaluate the impact of including the effects of radiation in the decay of the hadronically decaying W bosons, as the corresponding option is not supported for the dynamic scale chosen.

The MCFM cross sections are only used to evaluate the systematic uncertainties as detailed above and not to normalize the samples discussed in this section. Since the generators of these samples already have NLO accuracy themselves, their native cross sections are used.

6.3.2 Explicit variations for the Sherpa samples

Explicit scale variations have been generated for each of the semi-leptonic diboson final states. These include variations of the factorization scale μ_f, the renormalization scale μ_r as well as the resummation scale μ_q – each by a factor of 2 and 0.5, respectively. The cross sections for these alternative samples are given in table 7.

Table 7: Summary of the generator cross sections at $\sqrt{s}$ = 13 TeV predicted by Sherpa for various scale variations in semi-leptonic diboson final states. A dash indicates that the samples were still in production at the time of writing. The normalization of the Sherpa predictions includes a correction to account for different electroweak scheme (details are provided in section 6.2.1).

		Predicted cross sections
Final state	Scales setup	Sherpa (pb)
$W(\to \ell\nu)W(\to qq)$	$2\mu_f$	45.903
$W(\to \ell\nu)W(\to qq)$	$0.5\mu_f$	44.536
$W(\to \ell\nu)W(\to qq)$	$2\mu_r$	40.934
$W(\to \ell\nu)W(\to qq)$	$0.5\mu_r$	51.905
$W(\to \ell\nu)W(\to qq)$	$2\mu_q$	44.388
$W(\to \ell\nu)W(\to qq)$	$0.5\mu_q$	45.566
$W(\to \ell\nu)Z(\to qq)$	$2\mu_f$	10.587
$W(\to \ell\nu)Z(\to qq)$	$0.5\mu_f$	10.331
$W(\to \ell\nu)Z(\to qq)$	$2\mu_r$	9.272
$W(\to \ell\nu)Z(\to qq)$	$0.5\mu_r$	12.236
$W(\to \ell\nu)Z(\to qq)$	$2\mu_q$	10.251
$W(\to \ell\nu)Z(\to qq)$	$0.5\mu_q$	10.573
$Z(\to \ell\ell)W(\to qq)$	$2\mu_f$	3.155
$Z(\to \ell\ell)W(\to qq)$	$0.5\mu_f$	3.080
$Z(\to \ell\ell)W(\to qq)$	$2\mu_r$	2.766
$Z(\to \ell\ell)W(\to qq)$	$0.5\mu_r$	3.651
$Z(\to \ell\ell)W(\to qq)$	$2\mu_q$	3.059
$Z(\to \ell\ell)W(\to qq)$	$0.5\mu_q$	3.152
$Z(\to \nu\nu)W(\to qq)$	$2\mu_f$	6.228
$Z(\to \nu\nu)W(\to qq)$	$0.5\mu_f$	6.090
$Z(\to \nu\nu)W(\to qq)$	$2\mu_r$	5.453
$Z(\to \nu\nu)W(\to qq)$	$0.5\mu_r$	7.217
$Z(\to \nu\nu)W(\to qq)$	$2\mu_q$	6.055
$Z(\to \nu\nu)W(\to qq)$	$0.5\mu_q$	6.226
$Z(\to \ell\ell)Z(\to qq)$	$2\mu_f$	2.171
$Z(\to \ell\ell)Z(\to qq)$	$0.5\mu_f$	2.108
$Z(\to \ell\ell)Z(\to qq)$	$2\mu_r$	1.994
$Z(\to \ell\ell)Z(\to qq)$	$0.5\mu_r$	2.325
$Z(\to \ell\ell)Z(\to qq)$	$2\mu_q$	2.099
$Z(\to \ell\ell)Z(\to qq)$	$0.5\mu_q$	2.198
$Z(\to \nu\nu)Z(\to qq)$	$2\mu_f$	—
$Z(\to \nu\nu)Z(\to qq)$	$0.5\mu_f$	—
$Z(\to \nu\nu)Z(\to qq)$	$2\mu_r$	—
$Z(\to \nu\nu)Z(\to qq)$	$0.5\mu_r$	—
$Z(\to \nu\nu)Z(\to qq)$	$2\mu_q$	—
$Z(\to \nu\nu)Z(\to qq)$	$0.5\mu_q$	—

6.4 Generator comparisons

In the following we provide particle-level validation plots with different object definitions and event selections. Electrons and muons with $p_{\mathrm{T}} > 7$ GeV and within $|\eta| < 2.47$ (for electrons) or $|\eta| < 2.7$ (for muons) are considered in this study if the p_{T} sum of all charged particles (excluding the lepton candidate) within a cone of $\Delta R = 0.2$ around the lepton is less than 10 % of the lepton p_{T}. These are referred to as 'loose' selection criteria. Leptons passing 'medium' selection criteria are required to have $p_{\mathrm{T}} > 25$ GeV in addition to passing the loose selection. For leptons passing 'tight' selection criteria the isolation cut is reduced to 4 % in addition to passing the medium selection.

Where jets are used, they are reconstructed using the anti-k_t clustering algorithm [27] with a jet-radius parameter of $R = 0.4$. The jet transverse momentum is required to be greater than 20 GeV for central jets ($|\eta| < 2.5$) and greater than 30 GeV for forward jets ($2.5 < |\eta| < 5$). Jets with $|\eta| > 5$ are ignored. An overlap removal procedure is applied between selected jets and leptons. A jet is rejected if an electron passing the loose identification criteria can be matched to it in η-ϕ space ($\Delta R = 0.4$). Similarly a muon-jet overlap removal procedure is applied, provided that at most three charged particle tracks are pointing to the primary vertex associated with an overlapping muon candidate. Selected central jets passing the overlap-removal requirements are b-tagged if a B-hadron is found within a cone of $\Delta R = 0.3$ centered along the jet axis.

Further details of the selections are given in the respective subsections.

6.4.1 $W(\to \ell\nu)W(\to qq)$ final state

The $W(\to \ell\nu)W(\to qq)$ phase space is defined as

- at least two central jets
- exactly one lepton (electron or muon) passing tight selection criteria
- no additional leptons passing the loose selection criteria

The leptonically decaying vector boson candidate is reconstructed from the selected lepton and the missing transverse energy $E_{\mathrm{T}}^{\mathrm{miss}}$. Figure 16 shows a comparison of predictions obtained with `Powheg+PYTHIA8` and `Sherpa` for this region of phase space. All distributions are normalized to the predicted cross section of their respective generator.

The predictions from `Powheg+PYTHIA8` and `Sherpa` for these final states are found to be in fairly good agreement. For variables less sensitive to the production of additional radiation (as for instance the p_{T} of the leptonically decaying vector boson, the invariant mass of the leading jets pair or the p_{T} of the leading jet) the two predictions are in agreement within the error bands obtained from the `Sherpa` scale variations. Looking at the p_{T} of the third jet, one can observe larger differences which are not covered by the scale variations, with a harder p_{T} spectrum for `Sherpa`. This is not completely unexpected given that `Sherpa` includes NLO matrix elements for configurations with up to one additional parton, whereas the `Powheg` prediction is only accurate to leading order for this configuration.

The uncertainty bands on the `Sherpa` prediction are smooth and fairly flat. They are dominated by variations of the renormalization scale. A dependence on the p_{T} spectra can be observed for the uncertainty bands, with larger uncertainties for higher values of the vector-boson p_{T}, for instance. Looking at the p_{T} spectrum of the first additional emission ($p_{\mathrm{T}}^{\mathrm{extra\,jet}}$), the uncertainties from the scale variations are, as

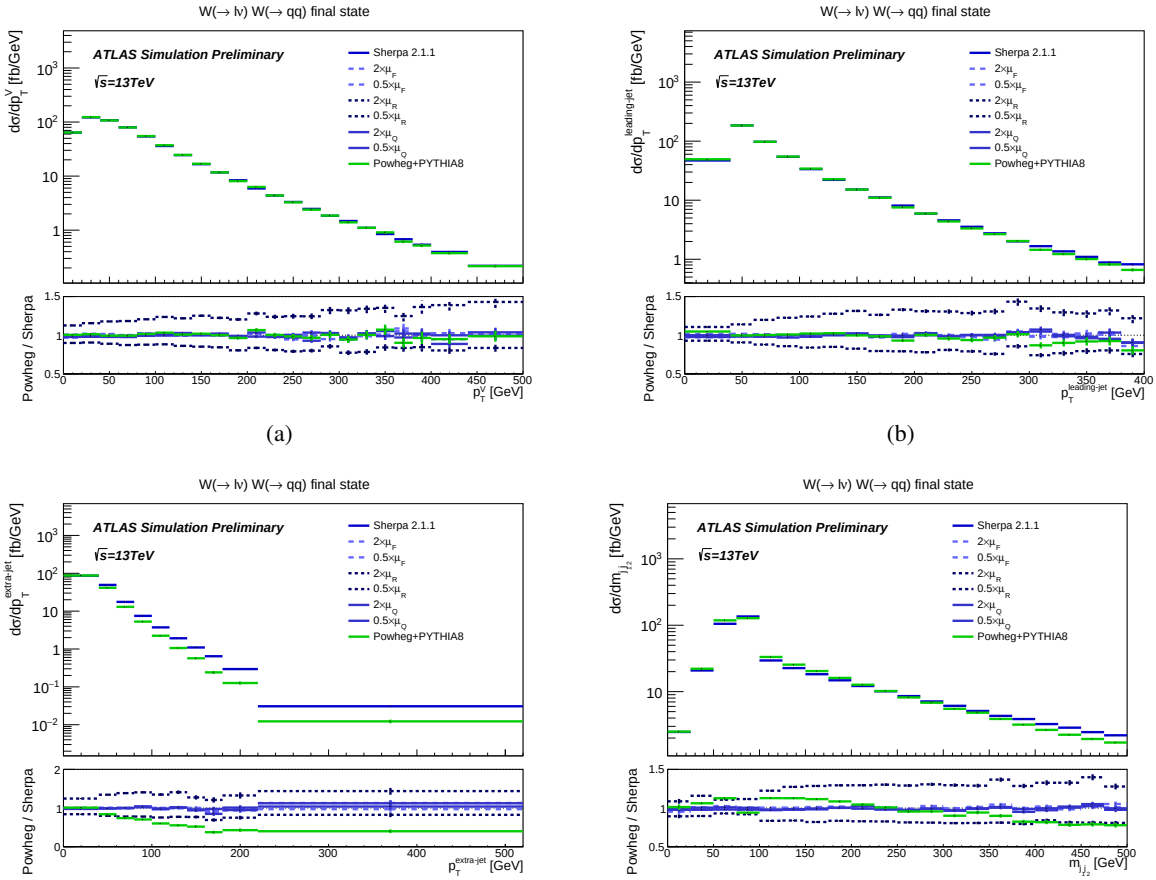

Figure 16: Comparisons of (a) the p_{T} of the leptonically decaying W-boson candidate, (b) the leading jet p_{T}, (c) the p_{T} of the third jet in p_{T} and as (d) the leading dijet invariant mass predicted by `Sherpa` (along with scale variations) as well as `Powheg+PYTHIA8` for $W(\rightarrow \ell\nu)W(\rightarrow qq)$ final states. The event selection has no b-tagging requirements on the selected jets.

expected, larger across the whole p_{T} range compared to the uncertainty bands for other more inclusive variables.

6.4.2 $W(\rightarrow \ell\nu)Z(\rightarrow qq)$ final state

The $W(\rightarrow \ell\nu)Z(\rightarrow qq)$ phase space is defined as

- at least two central jets
- exactly one lepton (electron or muon) passing tight selection criteria
- no additional leptons passing the loose selection criteria

The leptonically decaying vector boson candidate is reconstructed from the selected lepton and the missing transverse energy $E_{\mathrm{T}}^{\mathrm{miss}}$. Figure 17 shows a comparison of predictions obtained with `Powheg+PYTHIA8` and `Sherpa` for this region of phase space. All distributions are normalized to the predicted cross section of their respective generator.

The predictions from `Powheg+PYTHIA8` and `Sherpa` for these final states are found to be in fairly good agreement. For variables less sensitive to the production of additional radiation (as for instance the p_{T} of the leptonically decaying vector boson, the invariant mass of the leading jets pair or the p_{T} of the leading jet) the two predictions are in agreement within the error bands obtained from the `Sherpa` scale variations. Looking at the p_{T} of the third jet, one can observe larger differences which are not covered by the scale variations, with a harder p_{T} spectrum for `Sherpa`. This is not completely unexpected given that `Sherpa` includes NLO matrix elements for configurations with up to one additional parton, whereas the `Powheg` prediction is only accurate to leading order for this configuration.

The uncertainty bands on the `Sherpa` prediction are smooth and fairly flat. They are dominated by variations of the renormalization scale. A dependence on the p_{T} spectra can be observed for the uncertainty bands, with larger uncertainties for higher values of the vector-boson p_{T}, for instance. Looking at the p_{T} spectrum of the first additional emission ($p_{\mathrm{T}}^{\mathrm{extra\,jet}}$), the uncertainties from the scale variations are, as expected, larger across the whole p_{T} range compared to the uncertainty bands for other more inclusive variables.

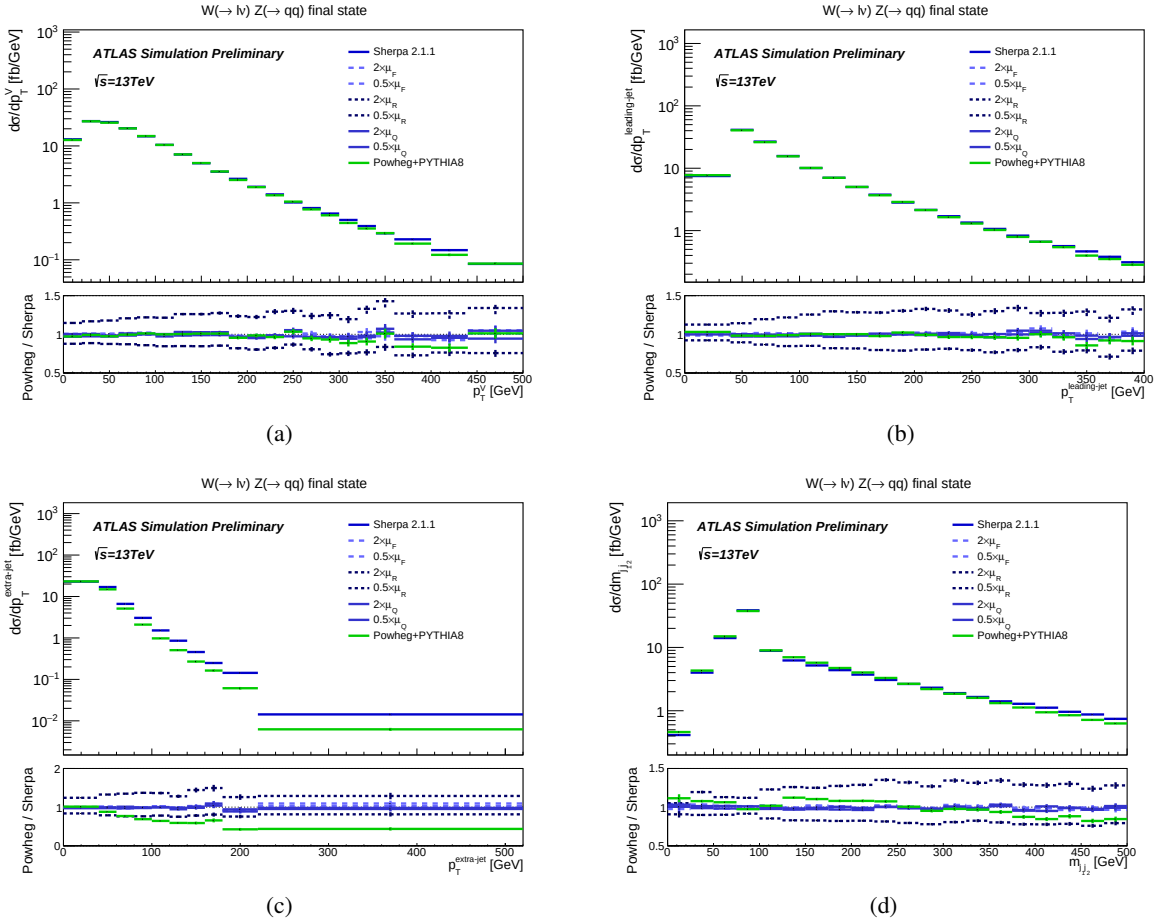

Figure 17: Comparisons of (a) the p_{T} of the leptonically decaying W-boson candidate, (b) the leading jet p_{T}, (c) the p_{T} of the third jet in p_{T} and (d) the leading dijet invariant mass predicted by `Sherpa` (along with its scale variations) as well as `Powheg`+`PYTHIA8` for $W(\rightarrow \ell\nu)Z(\rightarrow qq)$ final states. The event selection has no b-tagging requirements on the selected jets.

Figure 18 shows a comparison of predictions obtained with `Sherpa v2.1.1` and `Sherpa v2.2.0` for the same region of phase space. All distributions are normalized to the predicted cross section of their respective generator. It can be seen that the two versions of `Sherpa` agree quite well. The overall normalization difference between the two predictions is likely due to different acceptance effects from the applied selection cuts.

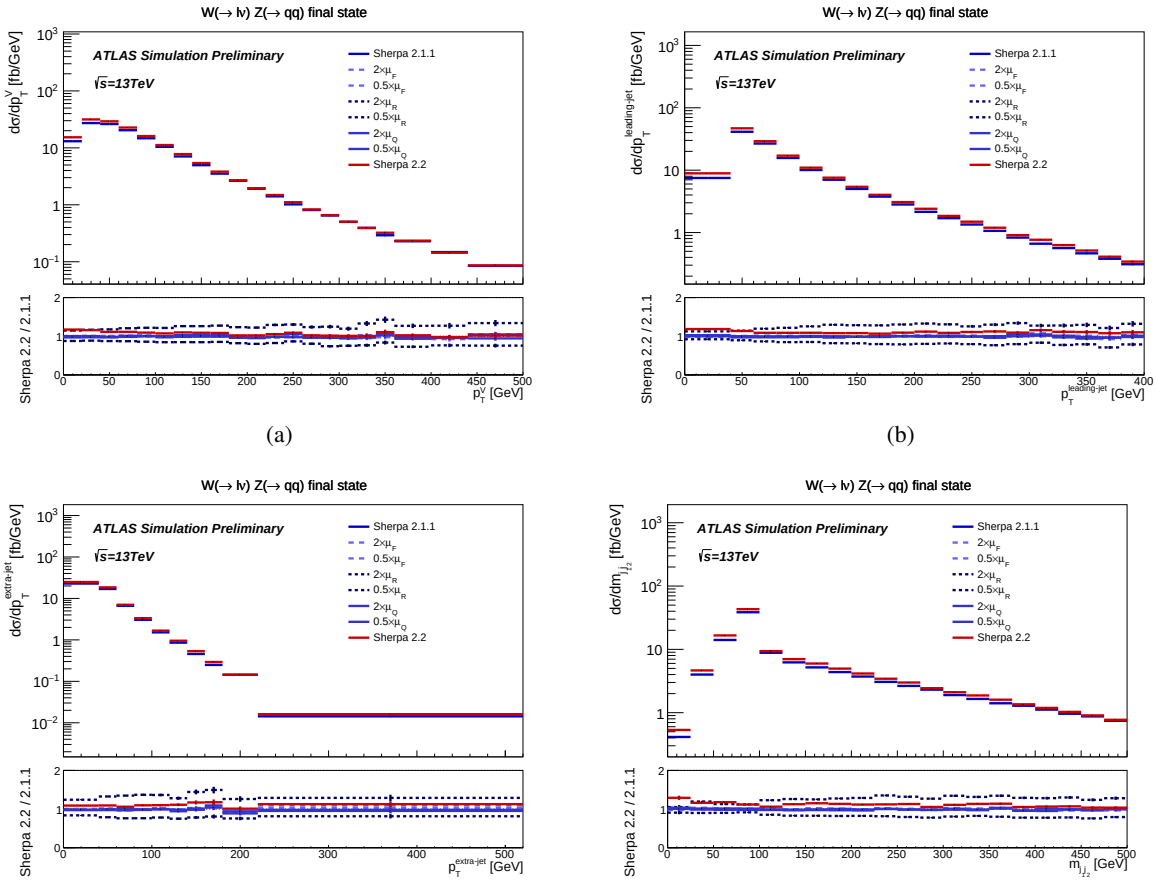

Figure 18: Comparisons of (a) the p_{T} of the leptonically decaying W-boson candidate, (b) the leading jet p_{T} (c) the p_{T} of the third jet in p_{T} and (d) the leading dijet invariant mass predicted by `Sherpa v2.1.1` (along with scale variations) as well as `Sherpa v2.2.0` for $W(\rightarrow \ell\nu)Z(\rightarrow qq)$ final states. The event selection has no b-tagging requirements on the selected jets.

6.4.3 $Z(\to \ell\ell)W(\to qq)$ final state

The $Z(\to \ell\ell)W(\to qq)$ phase space is defined as

- at least two central jets
- exactly two leptons (electrons or muons), at least one of which passing medium selection criteria
- no additional leptons passing the loose selection criteria

The leptonically decaying vector boson candidate is reconstructed from the selected leptons. Figure 19 shows a comparison of predictions obtained with `Powheg+PYTHIA8` and `Sherpa` for this region of phase space. All distributions are normalized to the predicted cross section of their respective generator.

The predictions from `Powheg+PYTHIA8` and `Sherpa` for these final states are found to be in fairly good agreement. For variables less sensitive to the production of additional radiation (as for instance the p_{T} of the leptonically decaying vector boson, the invariant mass of the leading jets pair or the p_{T} of the leading jet) the two predictions are in agreement within the error bands obtained from the `Sherpa` scale variations. Looking at the p_{T} of the third jet, one can observe larger differences which are not covered by the scale variations, with a harder p_{T} spectrum for `Sherpa`. This is not completely unexpected given that `Sherpa` includes NLO matrix elements for configurations with up to one additional parton, whereas the `Powheg` prediction is only accurate to leading order for this configuration.

The uncertainty bands on the `Sherpa` prediction are smooth and fairly flat. They are dominated by variations of the renormalization scale. A dependence on the p_{T} spectra can be observed for the uncertainty bands, with larger uncertainties for higher values of the vector-boson p_{T}, for instance. Looking at the p_{T} spectrum of the first additional emission ($p_{\mathrm{T}}^{\text{extra jet}}$), the uncertainties from the scale variations are, as expected, larger across the whole p_{T} range compared to the uncertainty bands for other more inclusive variables.

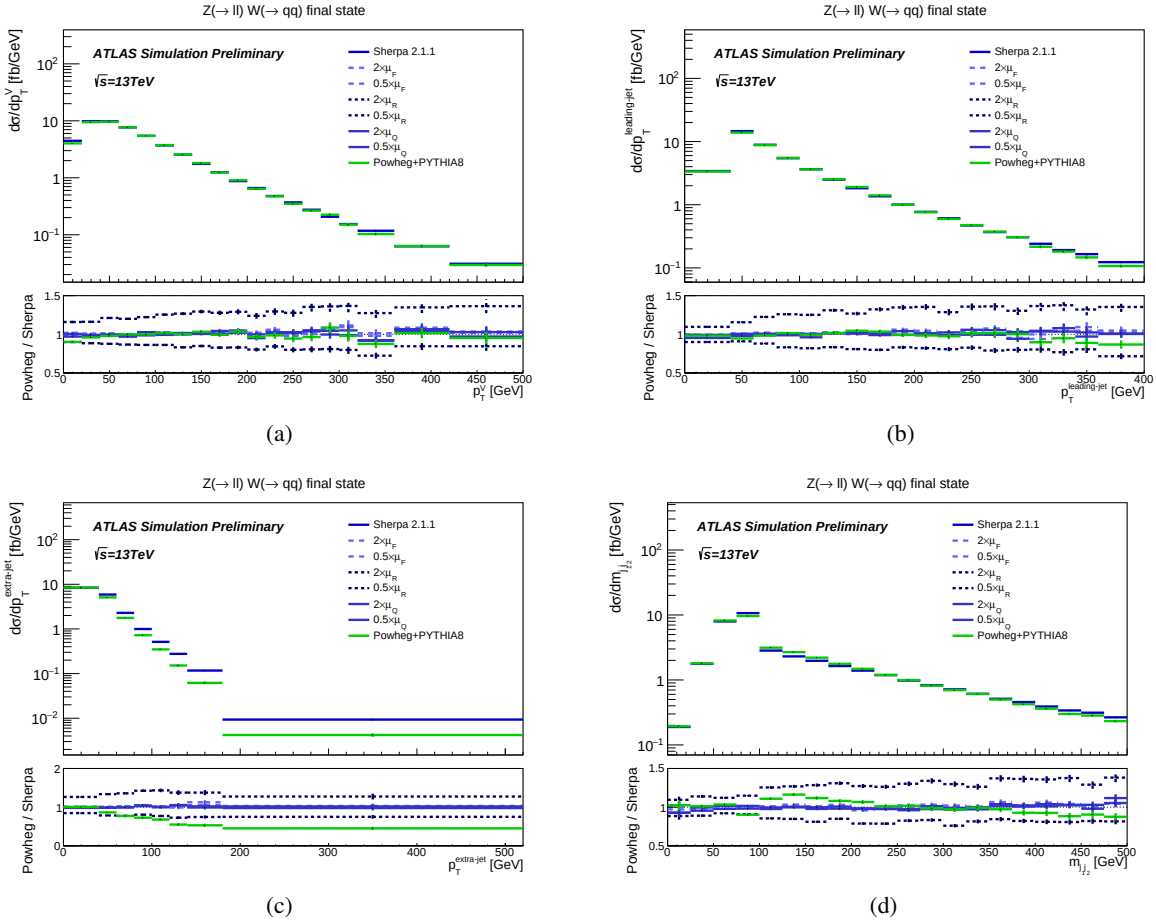

Figure 19: Comparisons of (a) the p_{T} of the leptonically decaying Z-boson candidate, (b) the leading jet p_{T}, (c) the p_{T} of the third jet in p_{T} and (d) the leading dijet invariant mass predicted by `Sherpa` (along with its scale variations) as well as `Powheg+PYTHIA8` for $Z(\rightarrow \ell\ell)W(\rightarrow qq)$ final states. The event selection has no b-tagging requirements on the selected jets.

6.4.4 $Z(\to \ell\ell)Z(\to qq)$ final state

The $Z(\to \ell\ell)Z(\to qq)$ phase space is defined as

- at least two central jets
- exactly two leptons (electrons or muons), at least one of which passing medium selection criteria
- no additional leptons passing the loose selection criteria

The leptonically decaying vector boson candidate is reconstructed from the selected leptons. Figures 20 and 21 show a comparison of predictions obtained with `Powheg+PYTHIA8` and `Sherpa` for this region of phase space, except that in the latter figure the two leading jets are also required to be b-tagged. All distributions are normalized to the predicted cross section of their respective generator.

The predictions from `Powheg+PYTHIA8` and `Sherpa` for these final states are found to be in fairly good agreement. For variables less sensitive to the production of additional radiation (as for instance the p_{T} of the leptonically decaying vector boson, the invariant mass of the leading jets pair or the p_{T} of the leading jet) the two predictions are in agreement within the error bands obtained from the `Sherpa` scale variations. Looking at the p_{T} of the third jet, one can observe larger differences which are not covered by the scale variations, with a harder p_{T} spectrum for `Sherpa`. This is not completely unexpected given that `Sherpa` includes NLO matrix elements for configurations with up to one additional parton, whereas the `Powheg` prediction is only accurate to leading order for this configuration.

Similar observations can be made for the phase space with the additional requirement of 2 b-tagged central jets (see figure 21), although in this case the statistics after applying the b-tagging selection requirement is substantially reduced, making detailed comparisons more difficult.

The uncertainty bands on the `Sherpa` prediction are smooth and fairly flat. They are dominated by variations of the renormalization scale. A dependence on the p_{T} spectra can be observed for the uncertainty bands, with larger uncertainties for higher values of the vector-boson p_{T}, for instance. Looking at the p_{T} spectrum of the first additional emission ($p_{\mathrm{T}}^{\mathrm{extra\,jet}}$), the uncertainties from the scale variations are, as expected, larger across the whole p_{T} range compared to the uncertainty bands for other more inclusive variables.

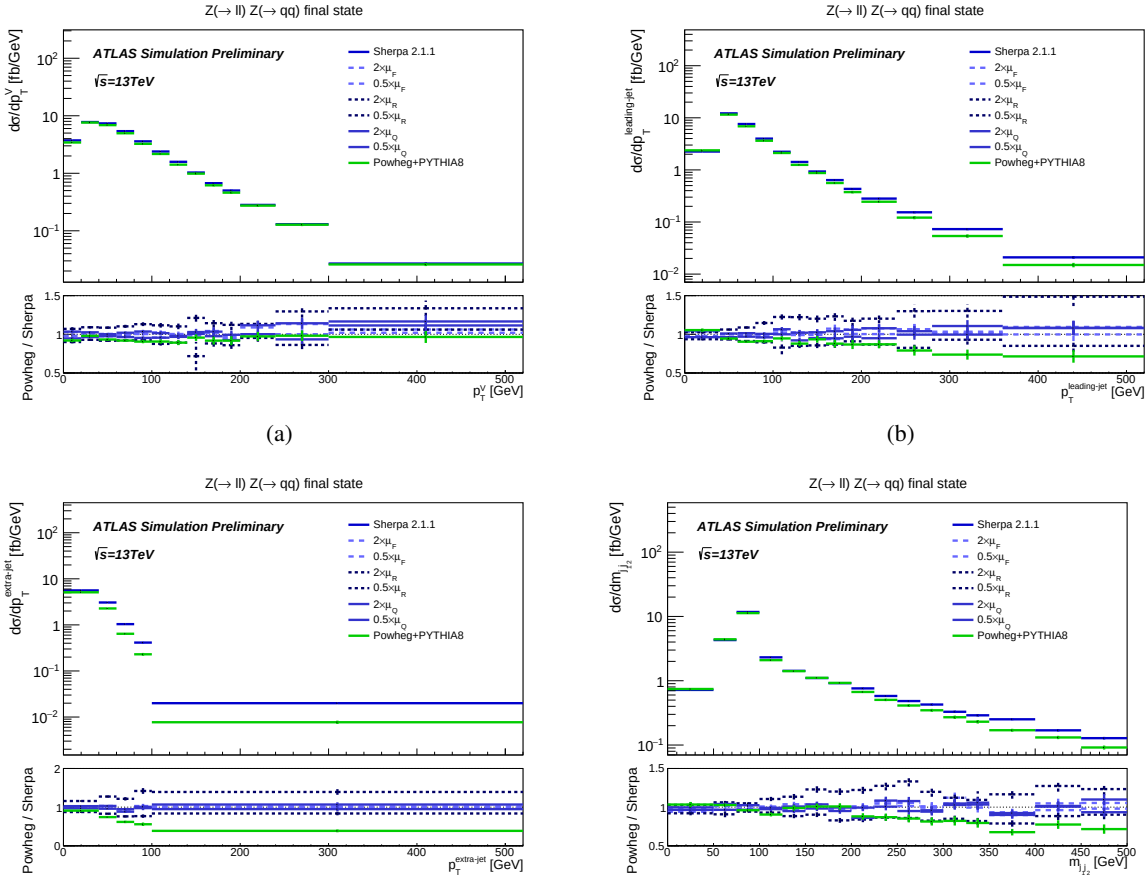

Figure 20: Comparisons of (a) the p_{T} of the leptonically decaying Z-boson candidate, (b) the leading jet p_{T}, (c) the p_{T} of the third jet in p_{T} and (d) the leading dijet invariant mass predicted by `Sherpa` (along with its scale variations) as well as `Powheg+PYTHIA8` for $Z(\rightarrow \ell\ell)Z(\rightarrow qq)$ final states. The event selection has no b-tagging requirements on the selected jets.

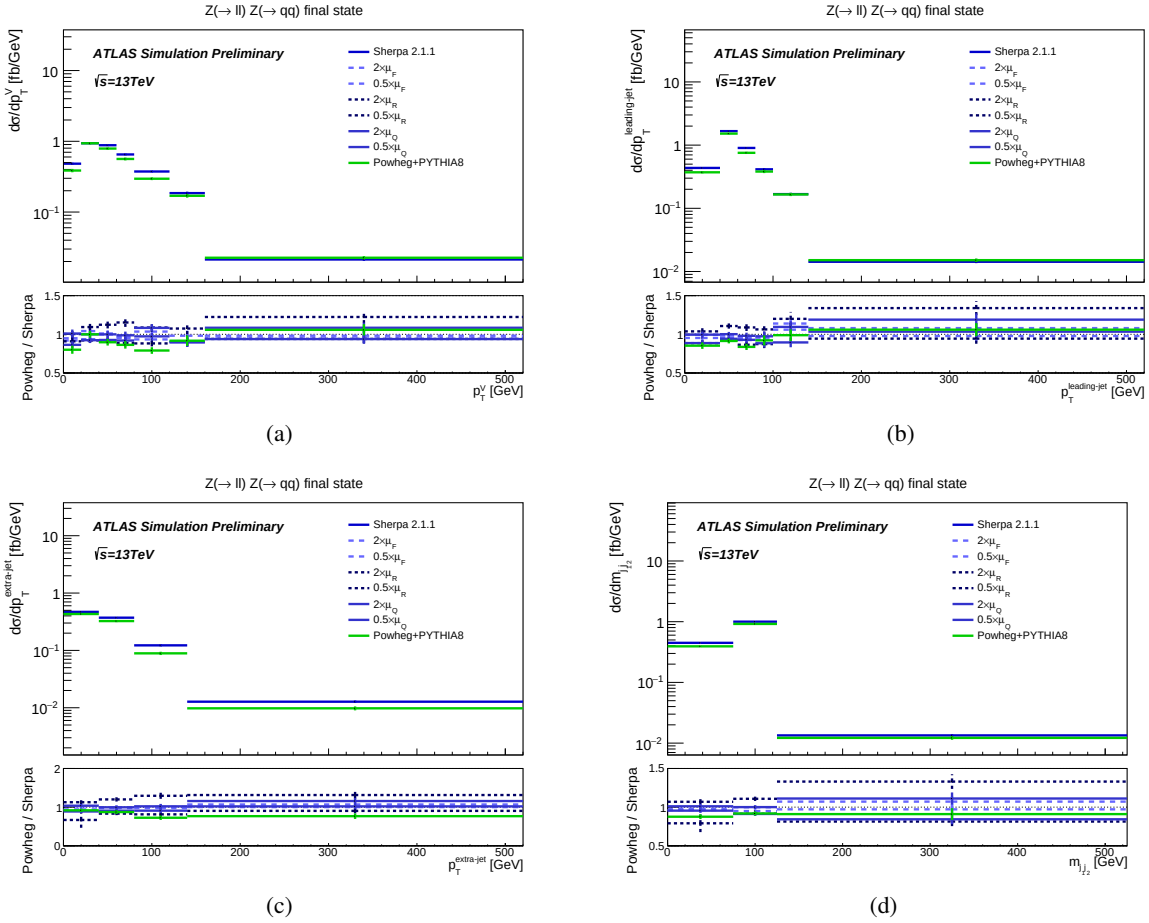

Figure 21: Comparisons of (a) the p_{T} of the leptonically decaying Z-boson candidate, (b) the leading jet p_{T}, (c) the p_{T} of the third jet in p_{T} and (d) the leading dijet invariant mass predicted by `Sherpa` (along with its scale variations) as well as `Powheg+PYTHIA8` for $Z(\rightarrow \ell\ell)Z(\rightarrow qq)$ final states. The event selection requires exactly 2 b-tagged jets among the selected central jets.

7 Triboson processes

7.1 Generator setup

7.1.1 Sherpa

Matrix elements for all combinations of $pp \to VVV$ with $V = W^{\pm}, Z$ have been generated using Sherpa v2.1.1 with up to two additional partons in the final state, including full NLO accuracy for the inclusive process. The setup is based on the one used in [32]. All diagrams with three electroweak couplings are taken into account, including diagrams involving Higgs propagators. But since these samples use factorized decays with on-shell vector bosons, the resonant contribution from those diagrams can not be reached from the 125 GeV Higgs. Processes with bottom quarks in the hard scattering process are ignored, to avoid contributions from top-quark mediated processes.

Leptonic decay channels have been enabled exclusively, using a factorized on-shell approach. The LO branching ratios are corrected to comply with the values given by the PDG [33]. No parton-level cuts are imposed on the generated phase space.

7.1.2 VBFNLO

The VBFNLO v2.7.0 Monte Carlo program [34–36] can generate vector boson fusion, double and triple vector boson production events at LO and it can also compute the corresponding process cross sections at NLO in QCD. VBFNLO is used to generate WWW events at LO using the CTEQ6L1 PDF and the dynamic scale of the mass of the three bosons for both the factorization and renormalization scales. The partonic events are processed by PYTHIA8 with the same PDF for parton showering. The A14 ATLAS tune [37] is used for the modeling of non-perturbative effects. The p_{T} of the three charged leptons in the final state is required to be greater than 5 GeV.

7.2 Cross sections

7.2.1 Generator cross sections

A summary of the cross sections predicted by Sherpa and VBFNLO is given in table 8. The Sherpa cross section is lower, because it is missing the contribution from on-shell Higgs-strahlung production due to the factorized decay setup.

Table 8: Summary of the generator cross sections at $\sqrt{s} = 13$ TeV predicted by Sherpa and VBFNLO for triboson final states. Note that the generator-level setup is not identical between the two, so some differences are expected.

	Predicted cross sections	
Final state	Sherpa (fb)	VBFNLO (fb)
ZZZ	0.316	—
ZZW	1.073	—
ZWW	5.164	—
WWW	8.330	11.03

7.3 Generator comparisons

7.3.1 $3\ell 3\nu$ final state

In the following, detector-level predictions are shown which originate from a background study performed in the context of the ATLAS search for supersymmetry in final states with jets and two same-sign leptons or three leptons [38]. The MC samples are processed through an ATLAS detector simulation [39] based on Geant4 [40] and are reconstructed in the same manner as the data. All predictions are normalized to a luminosity of 3.2 fb^{-1}.

The $WWW \to 3\ell 3\nu$ predictions by Sherpa and VBFNLO are compared after an event selection requiring at least 3 leptons with $p_{\mathrm{T}} > 10$ GeV with the leading two leptons required to have $p_{\mathrm{T}} > 20$ GeV. For VBFNLO the distributions are also shown after vetoing the Higgs contributions by rejecting the events with a W^+W^- pair with invariant mass in the 123–127 GeV range.

Although the chosen generators are expected to disagree to some extent due to the different accuracies of the calculations, it is still important to investigate the limitations of each setup in regions of phase space that analyses expect to be sensitive to, so as to be able to make an informed decision as to which of the available samples ought to be chosen.

Figure 22 shows selected lepton and jet distributions. Very good agreement is observed between both generators in terms of shapes after the Higgs contributions are removed in VBFNLO although as expected the normalization is lower. Larger differences are observed in jet distributions, with Sherpa predicting larger jet multiplicities (both with a threshold of $p_{\mathrm{T}} > 20$ GeV or $p_{\mathrm{T}} > 50$ GeV).

Figure 23 shows the comparison for global event observables, such as the $E_{\mathrm{T}}^{\mathrm{miss}}$ and the effective mass (m_{eff}) defined as the scalar sum of the p_{T} of the signal leptons and jets in the event plus the $E_{\mathrm{T}}^{\mathrm{miss}}$. Similar observations can be made in this case, with VBFNLO predicting softer $E_{\mathrm{T}}^{\mathrm{miss}}$ and m_{eff} distributions than Sherpa before subtracting the Higgs contributions, and much more similar shapes after these contributions are subtracted.

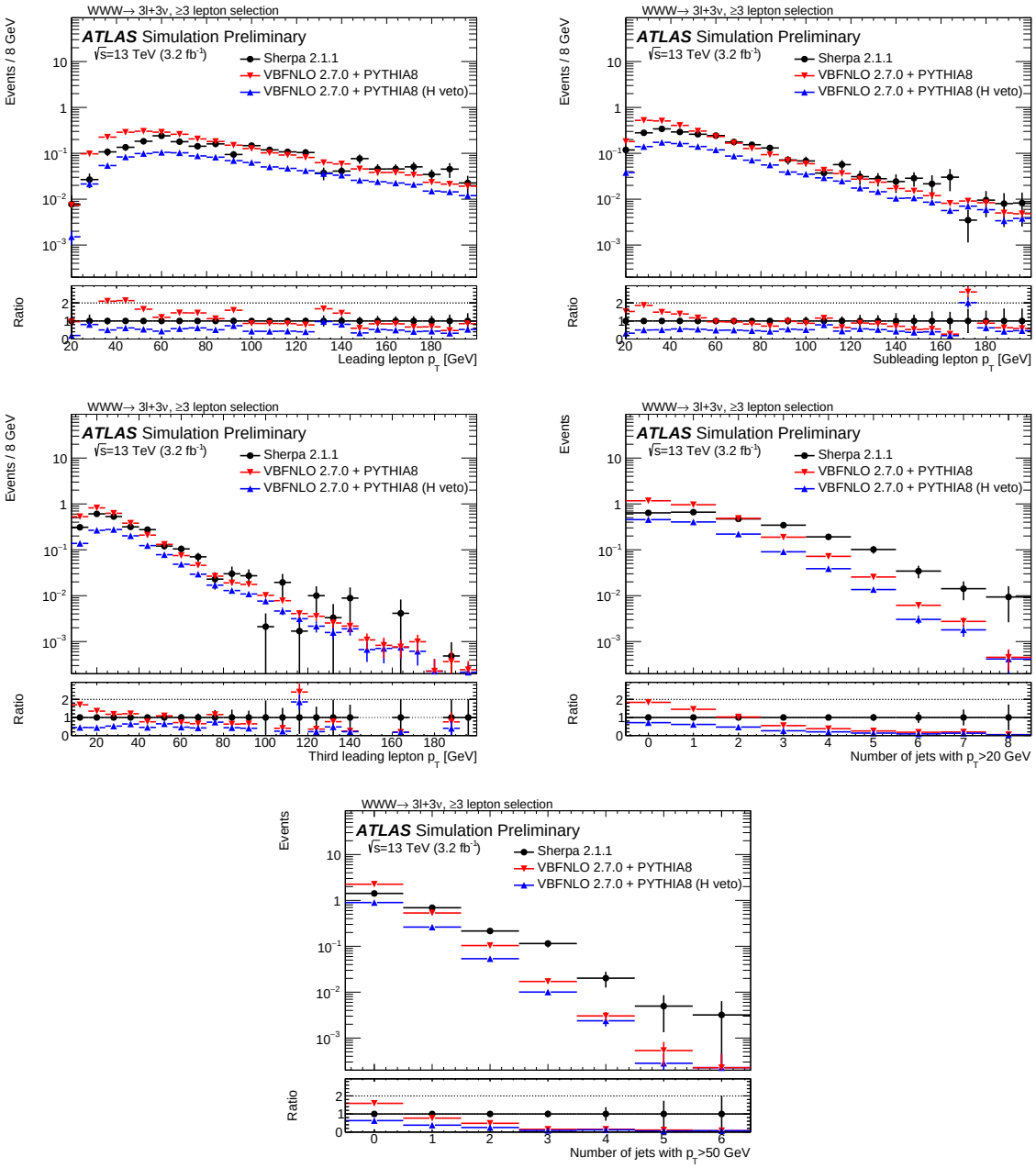

Figure 22: Several kinematic distributions for $WWW \to 3\ell 3\nu$ MC: p_{T} of the leading lepton (top left), sub-leading lepton (top right), third leading lepton (middle left), number of jets with $p_{\mathrm{T}} > 20$ GeV (middle right), number of jets with $p_{\mathrm{T}} > 50$ GeV (bottom). The predictions by `Sherpa` (in black) are compared with those by `VBFNLO` (in red) and by `VBFNLO` vetoing the Higgs contributions (in blue). The uncertainties are statistical only.

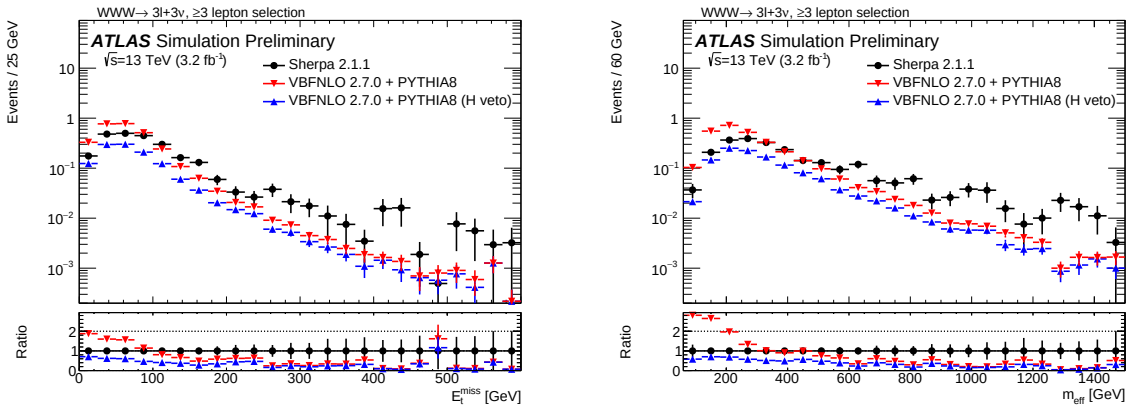

Figure 23: Distribution for the $E_{\mathrm{T}}^{\mathrm{miss}}$ (left) and effective mass (right) for $WWW \to 3\ell 3\nu$ MC. The predictions by `Sherpa` (in black) are compared with those by `VBFNLO` (in red) and by `VBFNLO` vetoing the Higgs contributions (in blue). The uncertainties are statistical only.

8 Conclusion

The Monte Carlo setup used by ATLAS to model multi-boson processes in 13 TeV pp collisions was described. State-of-the-art generators are utilized which were thoroughly validated and compared with each other in key kinematic distributions of the processes under study. Generally, good agreement is observed between the generators, or observed differences are understood based on the varying implementation of process features in the generators, such as the well-known forward activity excess in `Sherpa` as well as the insufficiency of the NLO+PS approach to adequately describe multi-jet configurations. A few differences remain to be clarified in collaboration with the theory community. The sample normalizations used by ATLAS were given as well and are generally based on the native generator cross-sections. Systematic uncertainties such as scale and PDF variations were described for the generators used as well as based on fixed-order cross section calculations to give an impact on sample normalization.

References

[1] T. Gleisberg et al., *Event generation with SHERPA 1.1*, JHEP **02** (2009) 007, arXiv: 0811.4622 [hep-ph].

[2] T. Gleisberg and S. Höche, *Comix, a new matrix element generator*, JHEP **0812** (2008) 039, arXiv: 0808.3674 [hep-ph].

[3] S. Schumann and F. Krauss, *A Parton shower algorithm based on Catani-Seymour dipole factorisation*, JHEP **03** (2008) 038, arXiv: 0709.1027 [hep-ph].

[4] S. Hoeche et al., *A critical appraisal of NLO+PS matching methods*, JHEP **09** (2012) 049, arXiv: 1111.1220 [hep-ph].

[5] S. Hoeche et al., *QCD matrix elements + parton showers: The NLO case*, JHEP **04** (2013) 027, arXiv: 1207.5030 [hep-ph].

[6] R. D. Ball et al., *Parton distributions for the LHC Run II*, JHEP **04** (2015) 040, arXiv: 1410.8849 [hep-ph].

[7] F. Cascioli, P. Maierhofer and S. Pozzorini, *Scattering Amplitudes with Open Loops*, Phys. Rev. Lett. **108** (2012) 111601, arXiv: 1111.5206 [hep-ph].

[8] A. Denner, S. Dittmaier and L. Hofer, *COLLIER - A fortran-library for one-loop integrals*, PoS **LL2014** (2014) 071, arXiv: 1407.0087 [hep-ph].

[9] H.-L. Lai et al., *New parton distributions for collider physics*, Phys. Rev. **D82** (2010) 074024, arXiv: 1007.2241 [hep-ph].

[10] P. Nason, *A New method for combining NLO QCD with shower Monte Carlo algorithms*, JHEP **11** (2004) 040, arXiv: hep-ph/0409146 [hep-ph].

[11] S. Frixione, P. Nason and C. Oleari, *Matching NLO QCD computations with Parton Shower simulations: the POWHEG method*, JHEP **11** (2007) 070, arXiv: 0709.2092 [hep-ph].

[12] S. Alioli et al., *A general framework for implementing NLO calculations in shower Monte Carlo programs: the POWHEG BOX*, JHEP **06** (2010) 043, arXiv: 1002.2581 [hep-ph].

[13] E. Boos et al., 'Generic user process interface for event generators', *Physics at TeV colliders. Proceedings, Euro Summer School, Les Houches, France, May 21-June 1, 2001*, 2001, arXiv: hep-ph/0109068 [hep-ph], URL: http://lss.fnal.gov/archive/preprint/fermilab-conf-01-496-t.shtml.

[14] J. Alwall et al., *A Standard format for Les Houches event files*, Comput. Phys. Commun. **176** (2007) 300, arXiv: hep-ph/0609017 [hep-ph].

[15] T. Sjöstrand et al., *An Introduction to PYTHIA 8.2*, Comput. Phys. Commun. **191** (2015) 159, arXiv: 1410.3012 [hep-ph].

[16] T. Melia et al., *W+W-, WZ and ZZ production in the POWHEG BOX*, JHEP **11** (2011) 078, arXiv: 1107.5051 [hep-ph].

[17] P. Nason and G. Zanderighi, W^+W^-, *WZ and ZZ production in the POWHEG-BOX-V2*, Eur. Phys. J. **C74**.1 (2014) 2702, arXiv: 1311.1365 [hep-ph].

[18] ATLAS Collaboration, *Measurement of the $Z/\gamma*$ boson transverse momentum distribution in pp collisions at $\sqrt{s}$ = 7 TeV with the ATLAS detector*, JHEP **2014** (2014) 55, arXiv: 1406.3660 [hep-ex].

[19] J. Pumplin et al., *New generation of parton distributions with uncertainties from global QCD analysis*, JHEP **07** (2002) 012, arXiv: hep-ph/0201195 [hep-ph].

[20] D. J. Lange, *The EvtGen particle decay simulation package*, Nucl. Instrum. Meth. **A462** (2001) 152.

[21] M. Grazzini, S. Kallweit and D. Rathlev, *ZZ production at the LHC: fiducial cross sections and distributions in NNLO QCD*, Phys. Lett. **B750** (2015) 407, arXiv: 1507.06257 [hep-ph].

[22] ATLAS Collaboration, *Measurement of the ZZ Production Cross Section in pp Collisions at $\sqrt{s}$ = 13 TeV with the ATLAS Detector* (2015), arXiv: 1512.05314 [hep-ex].

[23] J. M. Campbell and R. K. Ellis, *An Update on vector boson pair production at hadron colliders*, Phys. Rev. **D60** (1999) 113006, arXiv: hep-ph/9905386 [hep-ph].

[24] J. M. Campbell, R. K. Ellis and C. Williams, *Vector boson pair production at the LHC*, JHEP **07** (2011) 018, arXiv: 1105.0020 [hep-ph].

[25] J. M. Campbell, J. W. Huston and W. J. Stirling, *Hard Interactions of Quarks and Gluons: A Primer for LHC Physics*, Rept. Prog. Phys. **70** (2007) 89, arXiv: hep-ph/0611148 [hep-ph].

[26] A. D. Martin et al., *Parton distributions for the LHC*, Eur. Phys. J. **C63** (2009) 189, arXiv: 0901.0002 [hep-ph].

[27] M. Cacciari, G. P. Salam and G. Soyez, *The Anti-k(t) jet clustering algorithm*, JHEP **04** (2008) 063, arXiv: 0802.1189 [hep-ph].

[28] F. Cascioli et al., *Precise Higgs-background predictions: merging NLO QCD and squared quark-loop corrections to four-lepton + 0,1 jet production*, JHEP **01** (2014) 046, arXiv: 1309.0500 [hep-ph].

[29] N. Kauer and G. Passarino, *Inadequacy of zero-width approximation for a light Higgs boson signal*, JHEP **08** (2012) 116, arXiv: 1206.4803 [hep-ph].

[30] N. Kauer, *Interference effects for $H \to WW/ZZ \to \ell\bar{\nu}_\ell\bar{\ell}\nu_\ell$ searches in gluon fusion at the LHC*, JHEP **12** (2013) 082, arXiv: 1310.7011 [hep-ph].

[31] J. Bellm et al., *Herwig 7.0 / Herwig++ 3.0 Release Note* (2015), arXiv: 1512.01178 [hep-ph].

[32] S. Hoeche et al., *Triple vector boson production through Higgs-Strahlung with NLO multijet merging*, Phys. Rev. **D89**.9 (2014) 093015, arXiv: 1403.7516 [hep-ph].

[33] K. A. Olive et al., *Review of Particle Physics*, Chin. Phys. **C38** (2014) 090001.

[34] K. Arnold et al., *VBFNLO: A Parton level Monte Carlo for processes with electroweak bosons*, Comput. Phys. Commun. **180** (2009) 1661, arXiv: 0811.4559 [hep-ph].

[35] K. Arnold et al., *VBFNLO: A Parton Level Monte Carlo for Processes with Electroweak Bosons – Manual for Version 2.5.0* (2011), arXiv: 1107.4038 [hep-ph].

[36] J. Baglio et al., *Release Note - VBFNLO 2.7.0* (2014), arXiv: 1404.3940 [hep-ph].

[37] ATLAS Collaboration, *ATLAS Pythia 8 tunes to* 7 *TeV data*, ATL-PHYS-PUB-2014-021, 2014, URL: http://cdsweb.cern.ch/record/1966419.

[38] ATLAS Collaboration, *Search for supersymmetry at* $\sqrt{s} = 13$ *TeV in final states with jets and two same-sign leptons or three leptons with the ATLAS detector*, ATLAS-CONF-2015-078, 2015, URL: http://cdsweb.cern.ch/record/2114850.

[39] ATLAS Collaboration, *The ATLAS Simulation Infrastructure*, Eur. Phys. J. **C70** (2010) 823, arXiv: 1005.4568 [physics.ins-det].

[40] S. Agostinelli et al., *GEANT4: A Simulation toolkit*, Nucl. Instrum. Meth. **A506** (2003) 250.